UNIVERSITÀ DEGLI STUDI DI NAPOLI "FEDERICO II"

Dipartimento di Ingegneria Chimica, dei Materiali e della Produzione Industriale

Ph.D. IN MATERIALS AND STRUCTURES ENGINEERING

(XXVII CYCLE)

"Effect of density and interaction of surface-bound complexes on substrate-mediated delivery"

Tutor:

Prof. Paolo Antonio Netti

Candidate:

Dott.ssa Valeria Chianese

Coordinator:

Prof. Giuseppe Mensitieri

2012 – 2015

Table of Contents

ABSTRACT

Efficient and facile transfection of nucleic acids is a good tool for biological research and diagnostic applications. The crescent develop of gene transfer techniques for genomic studies, in particular has involved an increase of the investigations on gene transfer mediated by the substrate. This strategy is suitable for the manufacturing of screening platforms, such as microarrays, to *in vivo* and *in vitro* assays. Substrate-mediated transfection methods were described for delivering DNA in a slow release manner, but there is a critical need to modulate gene transfer process. In other words, a good gene delivery platform have to stably retain the gene vectors for prolonged periods and at same time mediate a efficient gene transfer when cells come in contact with it. To this address, we have investigated on different approaches of substrate-meditated delivery. In particular, have studied three kinds of interaction between gene vectors and substrate with the aim to find a compromise between the interaction strength and the effective gene transfer from substrate.

In the first instance, the process through which DNA-vectors were stably tethered to a glass substrate result inefficient to mediate the transfection, despite PEI/DNA complexes were internalized by the cells seeded on this functionalized substrates. We hypothesize that a low surface density of complexes, therefore an ineffective immobilization capability affect the subsequent gene transfer. Another factor be taken into account is the high co-localization of the internalized complexes with lysosomal compartments which suggests the likely involvement of a wrong mechanism of internalization by the cells placed on modified substrate.

Starting from this results, we have subsequently designed a substrate-mediate delivery with PEI/DNA complexes aspecifically adsorbed to glass slides. As expected, the successful transfection was probably affected by substrate release of the gene particles, as the quantification of the DNA/PEI complexes internalized by cells seeded on substrates in time indicates. In this case, in fact, there is not high lysosomal co-localization of the complexes inside cells on substrates.

At least, we have conduct a preliminary study with the aim to test a specific adsorption of gene particles to the substrate. To address this purpose we have investigated the binding affinity of a linker peptide to fibronectin coated substrate. Preliminary results confirm the specificity of selected peptide for the protein, in this way it will be possible adsorbed PEI/DNA complexes in specific way to a coated substrate, that simultaneously promotes cellular adhesion. This strategy to built a substrate-mediate gene delivery platform can be implement with the spatial protein patterning such as adhesive/transfective islands on substrate

Chapter 1

Introduction

1.1 Introduction

Gene expression within a cell population can be directly altered through gene delivery approaches, which have tremendous potential for therapeutically uses, such as gene therapy and tissue engineering, or in research and diagnostic applications, such as functional genomics. However a critical factor limiting the development of these applications is the inefficiency of gene transfer. The introduction of correctly functioning DNA into cells is a non-trivial matter, and cells must be coaxed to internalize, and then use, the DNA in the desired manner [1]. Direct injection of mg quantities of 'naked' DNA is usually well tolerated but still only yields very low levels of transfection. Since degradation of naked DNA by serum nucleases limits systemic administration, a number of polymer-based synthetic systems, or gene delivery vectors, have been developed in order to entice cells to use exogenous DNA and to enhance the stability of the delivered nucleic acids. Synthetic gene-delivery platforms have the intent to enhance the efficiency of gene transfer to the target cells and typically encompass three length scales - nano, micro and macro - depending on what is the desired cell type, anatomical site or diagnostic application [2]. Nanoscale delivery relates to vectors, which consist of nucleic acids packaged by proteins, lipids, or polymers. This complexation between nucleic acids and vectors produces small particles less negatively charged relative to the nucleic acid, protects against degradation and facilitates the intracellular trafficking. Most research efforts are focus on enhancing the efficacy of synthetic vectors to overcome one or more of the barriers to delivery. Microscale delivery vectors focus on the potential to deliver genes at a controlled rate for systemic uses. Delivery of the nucleic acid, indeed, requires to target a site of action, promote internalization by specific cell, escape from the endosome into the cytoplasm, transport into the nucleus for transcription, and ultimately protein production. Macroscale systems are two-dimensional (2D) or 3D scaffolds designed to deliver DNA to a population of cells proximal to the scaffold surface,

for tissue engineering and other applications [3, 4]. Biodegradable polymer scaffolds act as mechanical supports for initial growth of the cell seeded onto, and biomaterials can enhance gene transfer by maintaining consistent levels of the vector in the microenvironment of the cell [5]. However, cells in culture are generally grown on flat, 2D surfaces and represent an useful tool for cell-biology studies. Traditional delivery of vectors known as systemic or bolus delivery, leads to the presence of vector in the target cell population for a short time prior to clearance, aggregation, or degradation [6]. However DNA transfer to cells in culture can also be improved by DNA delivery from the cell growth substrate. These systems, termed substrate-mediated delivery, involve immobilization of either vectors to a surface that supports cell adhesion and control the rate at which plasmid DNA is delivered to the underside of cells grown at a solid or semi-solid interface. Substrate immobilization places the vector directly in the cellular microenvironment to reduce the amount of DNA required, preventing aggregation and distributing the DNA homogeneously among the cell population; it can potentially be used to spatially regulate gene transfer [7]. The immobilization of DNA to the surface can be through non-specifically adsorption, a receptor–ligand interaction, or by encapsulation within a matrix. One of the original reports focused on the development of microarrays to analyze the functions of specific gene-expression products [8]. On the other hand, a new strategy that uses the layer-by-layer approach to form multilayered polyelectrolyte thin films has been developed to incorporate and subsequently release DNA from a surface [9]. Other investigators have reported hybrid approaches where plasmid DNA, associated with gene vectors, was tethered to a surface to affect DNA delivery to the basal side of cells seeded to the surface [10, 11]. However, the success of research activity for gene delivery from 2D and 3D surfaces can be evaluated on a case-by-case basis.

1.2 Vectors for gene delivery

Although plasmid DNA provides transfection in vivo, packaging of nucleic acids with cationic lipids or polymers can facilitate uptake and increase expression of therapeutic gene or knockdown expression of a specific gene (i.e. RNAi) [12]. Complexation can support the uptake by enhancing interactions between positively charged DNA complexes and the negatively charged cellular membrane, in addition to providing stability against degradation. The success of gene delivery strongly depends on the use of vectors that could efficiently deliver the therapeutically active genes into the cells. Currently, vectors can be divided into two major groups, namely viral vectors derived from natural viruses and non-viral, synthetically manufactured vectors.

1.2.1 Viral vectors

Viral vectors are composed of either DNA or RNA surrounded by a capsid, since it is the nature of viruses to deliver their genes into host cells, they present good candidates for the development of effective gene delivery [13]. Natural evolution, however, optimized them for infecting and replicating their genome in host cells, but not necessarily for survival of the transduced cells or maintenance of the expressed genes. Nevertheless, replication-defective viruses, in which viral genes were partly replaced by therapeutic genes, were historically the first generation of 'viral vectors' applied in gene therapy. The common types of viruses used for gene delivery include retroviruses (which deliver RNA), adenoviruses (which deliver transiently expressing double-stranded DNA), and adeno-associated viruses (AAVs, which deliver single stranded stably expressing DNA). Viral particles range in size from 25 nm (AAVs) to 60–100 nm (adenoviruses and retroviruses) [2]. Other viruses that were used to develop viral vectors include herpes virus, pox virus, and more recently lentivirus. Viruses in general are highly efficient regarding

cellular uptake and intracellular delivery of therapeutic genes to the nucleus. To facilitate internalization, the virus surface can mediate binding to specific cell–surface receptors or to extra-cellular matrix molecules, which provides a natural corollary for substrate-mediated delivery [2]. Although, viral vectors provide the most efficient gene transfer among gene delivery vehicles, some viral vectors suffer from limitations on the gene size (36–38 kb) [14], others raise safety concerns [12, 15] as they have the potential to mutate or recombine with wild-type viruses or cause cellular damage, provoking an immune response that can lead to clearance of the vector or infected cells [16]. These potential issues have led to the exploration of non-viral delivery methods, which provide control over the chemical and physical properties of the vehicle.

1.2.2 Non-viral vectors

Non-viral vectors are attractive for their safety profiles and their synthetic design that allows high flexibility of the formulation that can be easily modified by diverse chemical reactions and physical interactions. However non-viral vectors yet yield lower efficiencies of gene transfer relative to viral vectors [2]. Non-viral vectors are more flexible in terms of type and size of the delivered nucleic acids. A broad range of nucleic acids from small double-stranded RNA for interfering with gene expression up to large artificial chromosomes can be used for transfection. The great advantage of non-viral vectors is their low immunogenicity, since synthetic vectors present far less or no immunogenic proteins or peptides in comparison to viral vectors. An obvious weakness of non-viral vectors is their low efficiency in intracellular nucleic acid delivery which currently is partly compensated by administration of large amounts of the vectors. DNA complexes are typically formulated by the self-assembly of plasmid, which are circular DNA molecules, with cationic lipids (to form lipoplexes) or polymers (to form polyplexes). Such compaction has been shown to protect the nucleic acids by providing a barrier

against nucleases, serum factors, and liver scavengers, thus limiting certain paths of DNA elimination from the body [17, 18]. The cationic agents bind to DNA or RNA due to electrostatic interactions and form particles of nanometer range. Indeed, complexes of cationic polymers, such as polyethylenimine (PEI) have mean diameters ranging from 100 nm to 1 μm, and zeta-potentials ranging from −14 mV to 21 mV. While, complexes formed with cationic lipids typically have mean diameters ranging from 200 nm to 1100 nm, with zeta-potentials that depend upon the cationic lipid [5]. The quantity of cationic lipid or polymer determines the properties of the complex; however, increasing the amount of lipid or polymer leads to cytotoxicity.

Mixing of DNA and cationic lipid results in the collapse of DNA to form a condensed structure—termed lipoplex—in which nucleic acids are buried within the lipid. The thermodynamic driving force for association of the DNA and lipid is the entropy increase from the release of counter ions and bound water associated with DNA and the lipid surface [19, 20]. The colloidal properties of lipoplexes are principally determined by the cationic lipid/DNA charge ratio, typically defined as the number of amines on the cationic lipid relative to the number of phosphate groups on the DNA [21]. The net charge on the lipoplex affects its interactions with other components present in vivo and in vitro (e.g. media, serum, extracellular matrix glycoproteins, mucosal secretions), which can limit the transfection efficiency. The main components of a cationic lipid are a hydrophilic lipid anchor, a linker group, and a positively charged headgroup. The lipid anchor is typically either a fatty chain or a cholesterol group, which determines the physical properties of the lipid bilayer, such as flexibility and the rate of lipid exchange [22]. The linker group is an important determinant of the chemical stability, biodegradability, and transfection efficiency of the cationic lipid. The positively charged headgroup on the cationic lipid is responsible for interacting with the negatively charged DNA and is a critical determinant of the transfection and cytotoxicity of liposome formulations, this cytotoxicity is believed to be attributable to lipid disruption of

the cellular and endosomal membranes. Lipoplexes have been formed from a variety of liposomal formulations, which often consist of a polyamine conjugated to a hydrophobic lipid tail [22]. The most used cationic lipids for gene delivery are DOTMA, DOTAP, and DOPE.

Cationic polymers, instead, contain high density of primary amines, which are protonable at neutral pH. This high density of positive charges allows the cationic polymers to form stable complexes with nucleic acids. In addition to proving positive charges for DNA complexation, the primary amines also serve as functional groups with which to chemical modify the polymers with ligand and peptides [23]. DNA polyplexes have been created with various cationic polymers including PLL [24], poly-L-histidine [25], poly-L-ornithine [25], and chitosan [26]. The most used cationic polymers for gene delivery are Poly-L-lysine (PLL) and Poly(ethylenimine) (PEI). In particular, complexation with polyethylenimine (PEI) has been considered the gold standard in polyplex-mediated gene transfer due to the ability of PEI–DNA complexes to transfect many cell types with high efficiency in vitro [27]. PEI is the organic macromolecule with the highest density of protonable amine functions and is therefore ideal to condense nucleic acids into particles of nanometer range [28]. The condensation process of DNA with the polycation PEI has been studied extensively. The particle size of DNA/PEI complexes depends on the molar ratio of PEI nitrogen to DNA phosphate (N/P ratio) and on the present salt concentration. Small individual particles are formed at low salt concentration (< 50 mM NaCl) and/or N/P ratios above 5, whereas formation of large aggregated particles is observed in the presence of salt (> 50 mM NaCl) at lower N/P ratios [29]. The net positive surface charge and an excess of free PEI during complex formation can prevent aggregation by repulsion of positive charges, whereas an increase in salt concentration reduces the hydration layer around the particles and promotes particle aggregation. However, PEI–DNA complexes have shown a limited ability to transfect certain types of cells,

furthermore PEI exhibits significant cytotoxicity both in vivo and in vitro [30, 31] and its non-biodegradability precludes repeated administration [32].

1.3 Intra- and extracellular barriers to gene transfer

For successful gene delivery, gene vectors must evade the immune system and be transported to the cell microenvironment for internalization. In particular, gene vectors have to overcome a series of barriers to gain access to the membrane surface, cytoplasmatic compartment, and nucleus of a target cell, and translate transgenes into protein. As particles encounter each of these barriers, they are subject to a certain probability of success or failure in overcoming each [33]. The *in vivo* delivery of viral vectors is strongly hampered by extracellular barriers, however, they are very efficient in overcoming intracellular barriers such as internalization into the host cell and delivery of the therapeutic gene towards the nucleus. In contrast, poor intracellular delivery of the carried nucleic acid remains the major barrier to effective gene transfer with non-viral vectors. In particular, the positive charge of lipoplexes and polyplexes enables interaction with the negatively charged cell-surface glycosaminoglycans and promotes passive cellular internalization [18, 23, 34]. Although positively charged vectors like PEI polyplexes expose high gene transfer activity in vitro systemic administration of such particles is rather restricted. In addition, gene transfer at effective DNA doses was associated with acute toxicity. *Ex vivo* experiments revealed that positively charged polyplexes induced aggregation of erythrocytes. These adverse effects can be overcome by ‘shielding’ of the positive surface charge of the vectors with hydrophilic polymers like polyethylene glycol (PEG). PEGylation of PEI polyplexes prevented erythrocyte aggregation, enhanced systemic circulation time and reduced toxicity of polyplexes [35]. Shielding with PEG, however, also

reduces the overall transfection efficiency because of reduced interaction with cell membranes of all cells including the target cells. After cellular association to the target cells, vectors particles are internalized by receptor-mediated endocytosis, macropinocytosis, phagocytosis or related processes [36]. The steps following internalization of DNA complexes, endosomal escape and nuclear localization, are thought to be rate limiting for the transfection of many cell types. Indeed, internalization of the plasmid does not necessarily correlate to transfection [37]. Internalized gene transfer complexes are mostly found in intracellular vesicles such as endosomes.[23] Entrapment in endosomes is thought to be associated with degradation of the complexes upon endosomal acidification. Therefore, subsequent release of particles into the cytoplasm represents a major bottleneck to gene delivery [38]. However, in many cases, the complexes are able to escape the endosome to be released to the cytosol [27, 34], where must subsequently avoid degradation and be transported to the nucleus for successful gene transfer.

For lipoplex-mediated delivery, the interaction of the lipids with the endosomal membrane is thought to facilitate escape of the DNA to the cytoplasm prior to its degradation in the lysosome. It is generally theorized that lipoplexes escape the endosome by destabilizing the membrane through structural changes and interactions of the liposomal amphiphiles with the endosomal membrane, thus enabling the DNA release to the cytosol [39]. Instead, it is hypothesized that polyplexes are able to escape the endosome via the "proton sponge effect," in which the buffering capacity of the cationic polymer leads to an osmotic pressure increase when the endosomal pH drops, ultimately causing the endosome to rupture and release the polyplexes to the cytosol [40]. PEI polyplexes and free PEI have considerable buffering capacity, because PEI is only partially protonated at physiological pH. Upon intracellular delivery of the DNA particle, the natural acidification within the endosome triggers protonation of complex-bound and free PEI, inducing chloride ion influx, osmotic swelling and destabilization of the vesicle which finally leads to release of the polyplexes into the cytoplasm [41].

However, this proton sponge effect is apparently not sufficient to release the majority of PEI particles from the vesicles. In particular, endosomal escape represents a major hurdle to efficient gene transfer with small PEI polyplexes at low concentrations [29]. After endosomal release DNA complexes or free DNA have to traffic through the cytoplasm towards the nucleus, enter the nucleus and expose the DNA to the cell's transcription machinery. This process is not clearly elucidated yet. Passive diffusion of DNA within the cytoplasm is restricted especially for larger plasmids [42], and free DNA can be degraded by nucleases within the cytoplasm. Therefore, the delivery of DNA towards the nucleus is supposed to depend mainly on the transport of intact complexes by microtubule or actin filaments [43]. The transport of DNA from the cytoplasm to the nucleus may be the most significant limitation to successful gene transfer. In addition to cytoplasmic transport limitations, the size of DNA is problematic for crossing into the nucleus. The nuclear pores allow free diffusion entry of only small particles ~ 70 kDa [44]. Nuclear import of DNA or DNA complexes is another big hurdle, it can be facilitated by the breakdown of the nuclear membrane, which is currently only easily during cell division [45]. Indeed, transfection of non-dividing cells with PEI polyplexes was several log units less effective compared to transfection of mitotic cells where the nuclear envelope was broken down [43].

1.4 Gene delivery systems

Success of gene delivery applications is supported by gene vectors that offer numerous advantages into overcome the intra-extracellular barriers. However, the transfection procedure itself can be a critical factor dictating the transfection efficiency. Currently most non viral gene delivery is conducted as a bolus delivery, which is the conventional transfection procedure that involves preplating cells, i.e., the cells are allowed to attach, recover, and grow for 24 h before transfection [46].

Systemic or bolus delivery, leads to the presence of vector in the target cell population for a short time prior clearance, aggregation, or degradation, which involve inefficient transfection due to mass transport issues and deactivation process [11]. Biomaterial-based delivery addresses extracellular barriers to enhance gene transfer, this delivery system can enhance gene transfer by maintaining consistent levels of the vector in the microenvironment of the cell and reducing the amount of DNA required, which can decrease cell toxicity. Numerous methods have been developed to provide controlled, localized, sustained, and triggered release of genes from biomaterials, overcoming these mass transport limitations [47-50]. These systems may be segregated into categories of gene activated matrices (GAMs), substrate-mediated delivery materials, and multilayered thin films.

1.4.1 Polymeric gene delivery

Incorporation of plasmids or particles within a polymeric scaffold or immobilization of these particles onto a surface can significantly limit the extracellular barriers to gene delivery [51]. In particular, polymeric gene delivery or GAMs has ability to provide control over the location and release profile of delivered genes. DNA encapsulation provides several advantages in comparison with bolus methods for gene delivery, such as protection of the DNA from extracellular barriers and degradation by serum nucleases and proteases [3]. This process thereby maintaining the bioactivity of the plasmid and the effective levels of the vector for prolonged times, extends the opportunity for cellular internalization and increases the likelihood of gene transfer [52]. The matrix also promotes the interactions between cells and plasmids , while simultaneously providing a 3D scaffold to maintain space [53, 54] and support the migration, proliferation, and differentiation of infiltrating cells. A critical aspect associated with the encapsulation of gene therapy vectors is that the matrix fabrication method

must be compatible with the vector integrity, indeed they can involve high temperatures, organic solvents, and the generation of free radicals or shear stresses that may damage the vector. Even if the vector is stably encapsulated, it can still be damaged by the degradation products. In these systems, where DNA was encapsulated, release may be accomplished by diffusion out of the scaffold and/or degradation of the matrix. As a result, the release profile can be tailored by varying the material such that the DNA is delivered rapidly as in bolus delivery or in a prolonged fashion over a period of months [54]. Sustained release formulations can compensate for vectors lost due to clearance or degradation. Delivery from most biomaterial systems likely occurs through a combination of vector interactions with the matrix and subsequent release, with the vector and material designed to regulate these interactions. Vector release from hydrophobic polymer scaffolds, for example, occurs by a sequence of polymer degradation, dissolution of the vector and subsequent diffusion from the polymer. While, the release from hydrophilic polymer scaffolds, hydrogels, has been modulated through modifying the hydrogel or vector chemistry. The mechanism of release can be, also, tuned to control whether the cells in the surrounding tissue or cells migrating into the matrix are targeted [53, 54]. In general, matrices that deliver via scaffold degradation limit gene transfer to cells that infiltrate the matrix [55], whereas diffusion-controlled methods maintain the ability to target cells in the vicinity of the matrix [56] due to the limited transport of DNA through tissue [57].

1.4.2 Substrate-mediated gene delivery

For many applications, the delivery inefficiencies may be overcome by surface immobilization of the vehicles. This delivery strategy, termed substrate-mediated delivery, solid phase delivery, or reverse transfection, mimics the natural process of virus binding to extracellular matrix proteins [56], immobilizing DNA-complexes to substrates and cells are then seeded onto these particles [51]. Placing the gene

vector directly within the cell's microenvironment, therefore overcoming diffusion and mass transport limitations associated with trafficking of nonviral complexes to cells [5]. In addition, surface immobilization of DNA–complexes has the ability to preserve complexes size observed in solution and inhibit complex aggregation, demonstrating that immobilization maintains vehicle activity [11] and reduces systemic removal, while cytotoxicity is reduced because less DNA is required to achieve gene transfer [10]. The preservation of vector activity and increased pDNA concentration in the cellular microenvironment elevates the efficiency of gene transfer, facilitating transgene expression levels comparable to or better than those achieved with bolus delivery, while delivering lower quantities of surface-immobilized pDNA [58]. Reverse transfection involves simultaneously transfecting and plating cells, almost similar to procedures used for transfecting suspension cells. Ziauddin and Sabatini were the first to report a method for reverse transfection16, this process as compared with conventional transfection allows rapid parallel analysis of large number of genes simultaneously. Finally, substrate-mediated delivery offers the ability to pattern the immobilization of nonviral complexes on surfaces, which can lead to patterned transgene expression, which is particularly pertinent to tissue engineering applications [51]. For substrate-mediated delivery, the properties of the surface are critical to both immobilization strategies and transfection (gene transfer) efficiencies. Different strategies have been proposed for reverse transfection methods. Surface immobilization typically employs either sequential deposition of DNA or cationic lipids and polymers, or the adsorption of preformed DNA complexes. Initial approaches immobilized DNA at the surface by entrapment within gelatin, followed by the addition of the transfection reagent.10 Subsequently, the transfection reagent has been initially adsorbed to the surface, followed by addition of the DNA. 11 This latter approach can be extended to the adsorption of multilayer films that gradually erode to expose the DNA for transfection[9]. Alternatively, the vectors can be formed in solution

and subsequently immobilized to the substrate, it can potentially be used to spatially regulate gene transfer.

1.4.3 Multilayered thin films

Multilayered thin films can both provide localized delivery of plasmids in vivo [59-65] and significantly sustain the release of a plasmid. These films have been created using many polyelectrolytes including PLL, PGA, chitosan, hyaluronan (HA), poly-(allylamine hydrochloride) (PAH), poly-(sodium-4-styrenesulfonate) (PSS) [66], and b-cyclodextrin [67], by alternately immersing a surface in a solution of a cationic molecule and in a solution of an anionic molecule in a process known as layer-by-layer (LbL) assembly [68-71]. The use of aqueous-based fabrication techniques in LbL assembly prevents the need for arduous wash steps to remove organic solvents [68]. Methods for the alternating, layer-by-layer adsorption of oppositely charged polymers on surfaces provide a practical approach to fabricate films using a broad range of naturally occurring and biologically important polyelectrolytes, including DNA, often without loss of biological function [72]. This general approach offers precise control over the compositions and thicknesses of thin polyelectrolyte-based films. Gene delivery from thin films containing plasmids has been engineered through the use of materials that degrade or disassemble under physiological conditions [73]. These nanometer-scale films were able to spatially and temporally control the gene delivery of multiple DNA constructs to promote transgene expression in vitro with various cell lines [68]. A recent and interesting approach toward thin film disassembly and plasmid release involves the alteration of the charge of the assembled cationic polymers. Thus, multilayered thin films are capable of promoting sustained release of plasmids from a substrate via multiple types of degradative processes.

1.5 Surface interactions

1.5.1 Non specific interactions

Vector immobilization to the biomaterial surface occurs through a combination of nonspecific and specific interactions that can be regulated through the design of the material and the vector. Molecular interactions between the vector and the polymer dictate whether the vector will be bound or released. Non specific immobilization approaches typically utilize the interaction of pDNA with cationic agents, which have shown the ability to promote localized gene delivery and sustained release. Viral and non-viral vectors, which contain negatively charged DNA or RNA potentially complexed with proteins, cationic polymers, or cationic lipids, interact with polymeric biomaterials through non-specific mechanisms, including hydrophobic, electrostatic, and van der Waals interactions that have been well characterized for adsorption and release of proteins from polymeric systems [74]. Many materials support the adsorption of proteins to the surface, and delivery vectors can adsorb directly to the substrate or to the proteins that are coating the surface. Complexes adsorbed to the substrate were homogeneously distributed across the surface. Based on protein adsorption,9 vector adsorption to biomaterials may be characterized by (1) changes in the hydration of the surface and vector, (2) charge interactions between the vector and the surface, (3) structural rearrangement of the adsorbing vector, and (4) the solution properties from which the complexes adsorb. Conformational changes in the vector may contribute to irreversible binding that limits cellular uptake, while hydrophilic substrates, which generally result in reversible interactions for proteins, may facilitate cellular internalization.2 Transgene expression by nonspecific immobilization of preformed complexes is dependent on the molecular composition of the vector, and the relative quantity of each vector component (e.g. of amines on the polymer to phosphate in DNA (N/P).

The quantity of immobilized complexes depended upon the charge and size of the DNA complexes. Transgene expression was observed on all substrates; however, the extent of transgene expression and the number of transfected cells were enhanced by precoating the substrate with serum proteins. This surface coating enabled homogeneously distributed complexes to redistribute to the cell surface.

1.5.2 Specific interaction

Strategies for specific immobilization include the use of complementary functional groups on the vector and surface, such as antigen-antibody interactions or biotin-avidin interactions [10], to control vector binding to the substrate. Upon complexation, a fraction of these functional groups will be available on the exterior of the particle for immobilization. Similarly, viral particles can be genetically engineered with specific sequences for binding or chemically modified after formation [75]. Indeed, viral vectors have been designed that specifically interact with natural and synthetic biomaterials through the use of antibodies or covalent coupling to allow for site-specific gene delivery. Although the functional groups provide specific interactions between the biomaterial and vector, nonspecific interactions contribute to vector immobilization [76]. The effective affinity of the vector for the biomaterial is determined by the strength of these molecular interactions, which may also be influenced by environmental conditions (e.g., ionic strength, pH), binding-induced conformational changes, or vector unpacking. Biotinylated-PEI has been used to complex pDNA and sequester the complexes on avidin-functionalized surfaces. While these systems provide many delivery advantages, efficient transfection using these immobilized vehicles requires careful control to balance the binding of the vehicle to the substrate with the ability to release the vehicle for cellular uptake. The specific binding of avidin-modified materials to biotinylated vectors has allowed researchers to identify several key

design parameters for specific immobilization strategies. It was shown that increasing the number of biotin groups in the complex, either through increasing the number of biotin residues per polymer or increasing the percentage of biotinylated polymers in the complex, increased the binding of the complexes to the substrate; however, maximal transfection in vitro was achieved when only a small fraction of the polymer forming the complex contained biotin. Maximal binding occurs when there is a high affinity of the complex for the substrate, but this high affinity reduces transfection.18 Manipulation of the rate of vehicle release thus inherently requires alteration of the properties of the vehicle and/or substrate. Furthermore, release is not cell-specific, and will occur for any cell that comes into contact with the vehicle. Cellular internalization can occur through breaking of the linkage between the complex and substrate, degradation of the substrate, or disruption of the complex to allow for release.

1.7 Aim of work

Aim of the research object of this PhD thesis is designing a transfection platform for substrate-mediated delivery able to stably retain gene vectors and at same time mediate a efficient gene transfer. To do so the role of the interaction, in terms of strength and specificity, between PEI-DNA complexes and the substrate in substrate-mediated gene transfer has been investigated. The results of the research carried out have provided the feasibility of preparing substrate-mediated gene delivery platforms using different approaches. In particular they have highlighted the suitability of assemble, organize and present the DNA to the surface, promoting the internalization of DNA by cells in way that provide opportunities to enhance levels of surface-mediated cell transfection.

The first part of the research was devoted to realization of a platform for reverse transfection immobilizating DNA complexes on substrate through a covalent bond.

The occurrence of PEI/DNA complexes on substrate and cellular uptake were evaluated.

In the second part, based upon the results of the performed experiments, gene complexes were weakly tethered to obtain a compromise between a good efficiency of reverse transfection and the stability of gene vector on substrate. Indeed, DNA complexes have been electrostatically adsorbed at surface of the substrate for reverse transfection. In this case cellular uptake and transfection results indicate that the success of this system is due to a release of gene complexes from the substrate.

The last part of the research, has been focused on the realization of a specific adsorption of gene particles to a protein-coated substrate. To this aim, a select peptide with effective affinity for fibronectin was evaluated as linker between coated substrate and PEI/DNA complexes. The efficiency of this system relate to the specificity with which PEI/DNA complexes interact with fibronectin coated substrate through this linker peptide is under evaluation. Furthermore, this strategy was implemented though the spatial protein patterning to create adhesive/transfective islands on substrate, for future application purposes.

1.8 References

1. Putnam, D., *Polymers for gene delivery across length scales.* Nature materials, 2006. **5**(6): p. 439-451.
2. Bengali, Z. and L.D. Shea, *Gene delivery by immobilization to cell-adhesive substrates.* MRS bulletin, 2005. **30**(09): p. 659-662.
3. Langer, R. and D.A. Tirrell, *Designing materials for biology and medicine.* Nature, 2004. **428**(6982): p. 487-92.
4. Niklason, L.E. and R. Langer, *Prospects for organ and tissue replacement.* JAMA, 2001. **285**(5): p. 573-6.
5. Bengali, Z., et al., *Gene delivery through cell culture substrate adsorbed DNA complexes.* Biotechnol Bioeng, 2005. **90**(3): p. 290-302.
6. Varga, C.M., K. Hong, and D.A. Lauffenburger, *Quantitative analysis of synthetic gene delivery vector design properties.* Mol Ther, 2001. **4**(5): p. 438-46.
7. Levy, R.J., et al., *Localized adenovirus gene delivery using antiviral IgG complexation.* Gene Ther, 2001. **8**(9): p. 659-67.
8. Ziauddin, J. and D.M. Sabatini, *Microarrays of cells expressing defined cDNAs.* Nature, 2001. **411**(6833): p. 107-10.
9. Zhang, J., L.S. Chua, and D.M. Lynn, *Multilayered thin films that sustain the release of functional DNA under physiological conditions.* Langmuir, 2004. **20**(19): p. 8015-21.
10. Segura, T. and L.D. Shea, *Surface-tethered DNA complexes for enhanced gene delivery.* Bioconjug Chem, 2002. **13**(3): p. 621-9.
11. Segura, T., M.J. Volk, and L.D. Shea, *Substrate-mediated DNA delivery: role of the cationic polymer structure and extent of modification.* J Control Release, 2003. **93**(1): p. 69-84.
12. Pannier, A.K. and L.D. Shea, *Controlled release systems for DNA delivery.* Mol Ther, 2004. **10**(1): p. 19-26.

13. De Laporte, L. and L.D. Shea, *Matrices and scaffolds for DNA delivery in tissue engineering.* Advanced drug delivery reviews, 2007. **59**(4): p. 292-307.
14. Cattaneo, R., et al., *Reprogrammed viruses as cancer therapeutics: targeted, armed and shielded.* Nat Rev Microbiol, 2008. **6**(7): p. 529-40.
15. Nazir, S.A. and J.P. Metcalf, *Innate immune response to adenovirus.* J Investig Med, 2005. **53**(6): p. 292-304.
16. Medzhitov, R. and C.A. Janeway, Jr., *Decoding the patterns of self and nonself by the innate immune system.* Science, 2002. **296**(5566): p. 298-300.
17. Boeckle, S., et al., *Purification of polyethylenimine polyplexes highlights the role of free polycations in gene transfer.* J Gene Med, 2004. **6**(10): p. 1102-11.
18. Mahato, R.I., L.C. Smith, and A. Rolland, *Pharmaceutical perspectives of nonviral gene therapy.* Adv Genet, 1999. **41**: p. 95-156.
19. Radler, J.O., et al., *Structure of DNA-cationic liposome complexes: DNA intercalation in multilamellar membranes in distinct interhelical packing regimes.* Science, 1997. **275**(5301): p. 810-4.
20. Bruinsma, F., S. Brown, and A. Venn, *The prevalence of prior infertility in recent mothers.* Aust N Z J Public Health, 1998. **22**(7): p. 841-2.
21. Xu, Y., et al., *Physicochemical characterization and purification of cationic lipoplexes.* Biophys J, 1999. **77**(1): p. 341-53.
22. Felgner, J.H., et al., *Enhanced gene delivery and mechanism studies with a novel series of cationic lipid formulations.* J Biol Chem, 1994. **269**(4): p. 2550-61.
23. Segura, T. and L.D. Shea, *Materials for non-viral gene delivery.* Annual Review of Materials Research, 2001. **31**(1): p. 25-46.
24. Kwoh, D.Y., et al., *Stabilization of poly-L-lysine/DNA polyplexes for in vivo gene delivery to the liver.* Biochim Biophys Acta, 1999. **1444**(2): p. 171-90.

25. Plank, C., et al., *Branched cationic peptides for gene delivery: role of type and number of cationic residues in formation and in vitro activity of DNA polyplexes.* Hum Gene Ther, 1999. **10**(2): p. 319-32.
26. MacLaughlin, F.C., et al., *Chitosan and depolymerized chitosan oligomers as condensing carriers for in vivo plasmid delivery.* J Control Release, 1998. **56**(1-3): p. 259-72.
27. Godbey, W.T., K.K. Wu, and A.G. Mikos, *Poly(ethylenimine) and its role in gene delivery.* J Control Release, 1999. **60**(2-3): p. 149-60.
28. Dunlap, D.D., et al., *Nanoscopic structure of DNA condensed for gene delivery.* Nucleic Acids Res, 1997. **25**(15): p. 3095-101.
29. Ogris, M., et al., *The size of DNA/transferrin-PEI complexes is an important factor for gene expression in cultured cells.* Gene Ther, 1998. **5**(10): p. 1425-33.
30. Hong, S., et al., *Interaction of polycationic polymers with supported lipid bilayers and cells: nanoscale hole formation and enhanced membrane permeability.* Bioconjug Chem, 2006. **17**(3): p. 728-34.
31. Breunig, M., et al., *Breaking up the correlation between efficacy and toxicity for nonviral gene delivery.* Proc Natl Acad Sci U S A, 2007. **104**(36): p. 14454-9.
32. Blocker, K.M., K.L. Kiick, and M.O. Sullivan, *Surface immobilization of plasmid DNA with a cell-responsive tether for substrate-mediated gene delivery.* Langmuir, 2011. **27**(6): p. 2739-2746.
33. Adler, A.F. and K.W. Leong, *Emerging links between surface nanotechnology and endocytosis: impact on nonviral gene delivery.* Nano Today, 2010. **5**(6): p. 553-569.
34. Niidome, T. and L. Huang, *Gene therapy progress and prospects: nonviral vectors.* Gene Ther, 2002. **9**(24): p. 1647-52.
35. Kircheis, R., et al., *Polycation-based DNA complexes for tumor-targeted gene delivery in vivo.* J Gene Med, 1999. **1**(2): p. 111-20.

36. Rejman, J., et al., *Size-dependent internalization of particles via the pathways of clathrin- and caveolae-mediated endocytosis.* Biochem J, 2004. **377**(Pt 1): p. 159-69.
37. Reimer, D.L., S. Kong, and M.B. Bally, *Analysis of cationic liposome-mediated interactions of plasmid DNA with murine and human melanoma cells in vitro.* J Biol Chem, 1997. **272**(31): p. 19480-7.
38. Zabner, J., et al., *Cellular and molecular barriers to gene transfer by a cationic lipid.* J Biol Chem, 1995. **270**(32): p. 18997-9007.
39. Hoekstra, D., et al., *Gene delivery by cationic lipids: in and out of an endosome.* Biochem Soc Trans, 2007. **35**(Pt 1): p. 68-71.
40. Boussif, O., et al., *A versatile vector for gene and oligonucleotide transfer into cells in culture and in vivo: polyethylenimine.* Proc Natl Acad Sci U S A, 1995. **92**(16): p. 7297-301.
41. Sonawane, N.D., F.C. Szoka, Jr., and A.S. Verkman, *Chloride accumulation and swelling in endosomes enhances DNA transfer by polyamine-DNA polyplexes.* J Biol Chem, 2003. **278**(45): p. 44826-31.
42. Suh, J., D. Wirtz, and J. Hanes, *Efficient active transport of gene nanocarriers to the cell nucleus.* Proc Natl Acad Sci U S A, 2003. **100**(7): p. 3878-82.
43. Brunner, S., et al., *Cell cycle dependence of gene transfer by lipoplex, polyplex and recombinant adenovirus.* Gene Ther, 2000. **7**(5): p. 401-7.
44. Jans, D.A., C.K. Chan, and S. Huebner, *Signals mediating nuclear targeting and their regulation: application in drug delivery.* Med Res Rev, 1998. **18**(4): p. 189-223.
45. Tseng, W.C., F.R. Haselton, and T.D. Giorgio, *Mitosis enhances transgene expression of plasmid delivered by cationic liposomes.* Biochim Biophys Acta, 1999. **1445**(1): p. 53-64.

46. Nimesh, S., et al., *Improved transfection efficiency of chitosan-DNA complexes employing reverse transfection.* Journal of Applied Polymer Science, 2012. **124**(3): p. 1771-1777.
47. Moses, J.W., et al., *Sirolimus-eluting stents versus standard stents in patients with stenosis in a native coronary artery.* N Engl J Med, 2003. **349**(14): p. 1315-23.
48. Stone, G.W., et al., *A polymer-based, paclitaxel-eluting stent in patients with coronary artery disease.* N Engl J Med, 2004. **350**(3): p. 221-31.
49. Saltzman, W.M. and W.L. Olbricht, *Building drug delivery into tissue engineering.* Nat Rev Drug Discov, 2002. **1**(3): p. 177-86.
50. Panyam, J. and V. Labhasetwar, *Biodegradable nanoparticles for drug and gene delivery to cells and tissue.* Adv Drug Deliv Rev, 2003. **55**(3): p. 329-47.
51. Pannier, A.K., B.C. Anderson, and L.D. Shea, *Substrate-mediated delivery from self-assembled monolayers: effect of surface ionization, hydrophilicity, and patterning.* Acta Biomaterialia, 2005. **1**(5): p. 511-522.
52. Wang, J., et al., *Synthesis and characterization of long chain alkyl acyl carnitine esters. Potentially biodegradable cationic lipids for use in gene delivery.* J Med Chem, 1998. **41**(13): p. 2207-15.
53. Shea, L.D., et al., *DNA delivery from polymer matrices for tissue engineering.* Nat Biotechnol, 1999. **17**(6): p. 551-4.
54. Bonadio, J., et al., *Localized, direct plasmid gene delivery in vivo: prolonged therapy results in reproducible tissue regeneration.* Nat Med, 1999. **5**(7): p. 753-9.
55. Doukas, J., et al., *Matrix immobilization enhances the tissue repair activity of growth factor gene therapy vectors.* Hum Gene Ther, 2001. **12**(7): p. 783-98.

56. Bajaj, B., P. Lei, and S.T. Andreadis, *High efficiencies of gene transfer with immobilized recombinant retrovirus: kinetics and optimization.* Biotechnol Prog, 2001. **17**(4): p. 587-96.

57. Zaharoff, D.A., et al., *Electromobility of plasmid DNA in tumor tissues during electric field-mediated gene delivery.* Gene Ther, 2002. **9**(19): p. 1286-90.

58. Luo, D. and W.M. Saltzman, *Enhancement of transfection by physical concentration of DNA at the cell surface.* Nat Biotechnol, 2000. **18**(8): p. 893-5.

59. Perlstein, I., et al., *DNA delivery from an intravascular stent with a denatured collagen-polylactic-polyglycolic acid-controlled release coating: mechanisms of enhanced transfection.* Gene Ther, 2003. **10**(17): p. 1420-8.

60. Klugherz, B.D., et al., *Gene delivery from a DNA controlled-release stent in porcine coronary arteries.* Nat Biotechnol, 2000. **18**(11): p. 1181-4.

61. Walter, D.H., et al., *Local gene transfer of phVEGF-2 plasmid by gene-eluting stents: an alternative strategy for inhibition of restenosis.* Circulation, 2004. **110**(1): p. 36-45.

62. Fishbein, I., et al., *Site specific gene delivery in the cardiovascular system.* J Control Release, 2005. **109**(1-3): p. 37-48.

63. Nakayama, Y., et al., *Development of high-performance stent: gelatinous photogel-coated stent that permits drug delivery and gene transfer.* J Biomed Mater Res, 2001. **57**(4): p. 559-66.

64. Klugherz, B.D., et al., *Gene delivery to pig coronary arteries from stents carrying antibody-tethered adenovirus.* Hum Gene Ther, 2002. **13**(3): p. 443-54.

65. Takahashi, A., et al., *Transgene delivery of plasmid DNA to smooth muscle cells and macrophages from a biostable polymer-coated stent.* Gene Ther, 2003. **10**(17): p. 1471-8.

66. Meyer, F., et al., *Polyplex-embedding in polyelectrolyte multilayers for gene delivery.* Biochim Biophys Acta, 2006. **1758**(3): p. 419-22.
67. Jessel, N., et al., *Multiple and time-scheduled in situ DNA delivery mediated by beta-cyclodextrin embedded in a polyelectrolyte multilayer.* Proc Natl Acad Sci U S A, 2006. **103**(23): p. 8618-21.
68. Jewell, C.M. and D.M. Lynn, *Multilayered polyelectrolyte assemblies as platforms for the delivery of DNA and other nucleic acid-based therapeutics.* Adv Drug Deliv Rev, 2008. **60**(9): p. 979-99.
69. Vazquez, E., et al., *Construction of hydrolytically-degradable thin films via layer-by-layer deposition of degradable polyelectrolytes.* J Am Chem Soc, 2002. **124**(47): p. 13992-3.
70. Wood, K.C., et al., *Controlling interlayer diffusion to achieve sustained, multiagent delivery from layer-by-layer thin films.* Proc Natl Acad Sci U S A, 2006. **103**(27): p. 10207-12.
71. Lowman, G.M., et al., *Novel solid-state polymer electrolyte consisting of a porous layer-by-layer polyelectrolyte thin film and oligoethylene glycol.* Langmuir, 2004. **20**(22): p. 9791-5.
72. Tang, Z., et al., *Biomedical Applications of Layer-by-Layer Assembly: From Biomimetics to Tissue Engineering.* Advanced Materials, 2006. **18**(24): p. 3203-3224.
73. Lynn, D.M., *Layers of opportunity: nanostructured polymer assemblies for the delivery of macromolecular therapeutics.* Soft Matter, 2006. **2**(4): p. 269-273.
74. Norde, W. and J. Lyklema, *Why proteins prefer interfaces.* J Biomater Sci Polym Ed, 1991. **2**(3): p. 183-202.
75. Barry, M.A., et al., *Biotinylated gene therapy vectors.* Expert Opin Biol Ther, 2003. **3**(6): p. 925-40.

76. Segura, T., P.H. Chung, and L.D. Shea, *DNA delivery from hyaluronic acid-collagen hydrogels via a substrate-mediated approach.* Biomaterials, 2005. **26**(13): p. 1575-84.

Chapter 2

Platform for gene delivery: covalent interaction between PEI/DNA complexes and cell-culturing glass substrate.

2.1 Introduction

In recent years, the development of systems capable of controlled and efficient gene transfer has concerned many in vitro research and diagnostic applications. In particular, gene delivery from surfaces is the basis of many screening systems to examine the cellular response to altered gene expression within a more representative biological context [1, 2]. Transfected cell arrays for studies in functional genomics [3-5] or patterned gene delivery for models of tissue growth [6, 7] are examples of applications of gene delivery studies to basic research. Substrate-mediated gene transfer, also known as reverse transfection, has the potential to retain for a long period of time effective DNA levels in a constrained area, avoiding the possibility of dispersion, extending the opportunity for cellular internalization and increasing the likelihood of gene transfer [8]. This delivery method involves the immobilization of DNA to a substrate that supports cell adhesion placing the vector directly in the cell microenvironment, reducing mass transport limitations and localizes delivery [9]. However, if the association of gene particles with a substrate is too tight, endocytic uptake and transfection can suffer [10]. In order to obtain a successful reverse transfection system, the interaction between substrate and gene vector must be sufficiently strong to immobilize and maintain the vector at the surface, while allowing for cellular internalization. Substrate and vector properties mediate the vector-surface interactions that are determinants of binding and gene transfer [11, 12]. The context wherein immobilized DNA-vector complexes are presented to cells can be modified with surface chemistry. A bioactive compound can be immobilize to a polymeric surface through various methods such as (i) adsorption via electrostatic interactions, in which complexes physically adsorbed onto the substrate were spontaneously and gradually desorbed from the surface during cell cultivation [13], (ii) ligand–receptor pairing, such as biotin–avidin, the strongest reported non-covalent bond [14] and (iii) covalent attachment. The latter offer several advantages by providing

the most stable bond between the compound and the functionalized polymer surface. The covalent immobilization of bioactive compounds has seen rapid grown in the past decade with applications in various fields [14, 15]. In the biomedical field, a covalent immobilization can be used to extend the half-life of a biomolecule or prevent its metabolism, as in compounds which provide anti-tumor activity when used locally, but may be toxic if metabolized [16]. Several polymers have been selected as substrates for biomolecule immobilization but, because of their inert nature, they must undergo surface functionalization, by introducing reactive functional groups, prior to attachment of a bioactive compound. Different surface modification strategies have been developed to improve wetting, adhesion, and printing of polymer surfaces by introducing a variety of polar groups, with little attention to functional group specificity. However, when surface modification is a precursor to attaching a bioactive compound, these techniques must be tailored to introduce a specific functional group [17]. Tethering a bioactive compound to a solid substrate via a spacer molecule, can also improve bioactivity by reducing steric constraints and shielding the compound from hydrophobic surface induced denaturation. In the same way, also binding of gene complexes to glass substrates for culturing cells requires surface modification. In particular, the covalent attachment of a bioactive compound to a glass surface involve glass pre-treatment and surface activation, commonly using silane [18]. Normally, vinyl silane or methacrylate silane was used as a coupling agent, because it contains at least one functional group with double bond, which can readily react with organic polymer, and functional groups that react with silanol groups on the glass surface [19]. It acts as a compound that provide at the interface of dissimilar materials in a composite, a stable bond resulting in improved composite properties and preservation of these properties.

In this chapter was investigated the stability and bioactivity of PEI/DNA complexes covalently bound to a glass substrates. In order to tether DNA complexes to glass slides, functional groups were introduced both on gene vector

and substrate. In particular, glass surface was activated with a methacrylate silane monolayer and PEI/DNA complexes were functionalized through modification of PEI molecules with acrylated PEG The changes of substrate and complexes properties were characterized and the occurrence of complexes on substrates after binding photoreaction was been investigated. Furthermore the efficiency of this system was evaluated respect to the cellular response to interaction with bound complexes.

2.2 Materials and Methods

2.2.1 Materials

Linear Polyethylenimine (L-PEI) with an average molecular weight of 25 kDa was purchased from Polysciences (Warrington, PA). Tetramethylrhodamine-conjugated linear PEI (JetPEI-fluoR) was purchased from Polyplus-transfection SA (7mM ammine content, Illkirch, France). Acryloyl-PEG-N-hydroxysuccinimmide (Ac-PEG-NHS, 3.4kDa) was purchased from Creative PEG Works (Winston-Salem, NC, USA). 3-aminopropyl triethoxysilane (APTES) and 3-(Trimethoxysilyl)propyl methacrylate (TMSPMA) were purchased from Sigma Aldrich (St. Louis, MO, USA). The reporter plasmid encoding for enhanced green fluorescent protein (p^{CMV}EGFP) driven by a cytomegalovirus (CMV) promoter was amplified in DH5α competent *Escherichia coli* strain, extracted and purified from bacterial culture using Qiagen plasmid kit (Santa Clara, CA) and stored in Tris-EDTA buffer solution. Transfection studies were performed with NIH/3T3 mouse fibroblasts cultured in a humidified 5 % CO_2 atmosphere at 37 °C in Dulbecco's modified Eagle medium with 4.5 g L^{-1} glucose (DMEM) (Gibco) supplemented with 10 % Bovine Calf Serum (BCS) (Gibco), 4 mM glutamine, 100 U mL^{-1} penicillin and 0.1 mg mL^{-1} streptomycin in a 100 mm diameter cell culture dish (Corning, NY, USA).

Plasmid DNA (p^{CMV}EGFP) was labeled with the cyanine dye Cy5 using Label IT® Tracker™ Intracellular Nucleic Acid Localization Kit purchased from Mirus Bio (Madison, WI, USA).

2.2.2 Plasmid DNA labeling

Plasmid DNA, p^{CMV}EGFP, was labeled with cyanine dye Cy5 using Label IT® Tracker™ Intracellular Nucleic Acid Localization Kit (Mirus Bio, Madison, WI, USA). Briefly, 20 µg of plasmid DNA was mixed with 10 µl of reagent in a total volume of 300 µl, followed by incubation for 1 h at 37 °C according to the recommendation by the supplier [20]. After 0.1 volumes of 5 M NaCl were added and Label IT reagent was removed by overnight precipitation with 2 volumes of ice-cold absolute ethanol at – 20 °C. The labeled DNA was recovered by centrifugation at 13,000 rpm for 15 minutes. The pellet was washed with 70% ethanol and resuspended in molecular biology grade water. The purity was monitored by measuring the ratio of absorbance at 260 nm and 280nm (A_{260nm}/A_{280nm}) at NanoDrop 2000 UV-Vis Spectrophotometer.

2.2.3 Synthesis of acryloyl-PEG-PEI conjugate

Ac-PEG-PEI copolymer was synthesized by combining 0.7 µmol of linear PEI (25 kDa, Polyscience) dissolved in 1 ml of 0.25 M NaCl with 0.8 ml of H_2O containing 2 µmol of acryloyl-PEG-N-hydroxysuccinimide (3.4 kDa, Creative PEG Works). The solution was magnetically stirred at room temperature overnight and subsequently loaded on a Macro-prep (Macro-prep High S; HR 10/10, BioRad, München, Germany) and fractionated with a salt gradient from 0.5 to 3.0 M NaCl in 20 mM HEPES at pH 7.1. The product was eluted between 2.4 and 2.9 ml M NaCl. The PEG-PEI conjugate was dialyzed against 2 l HBS (20 mM HEPES pH

7.3, containing 150 mM NaCl). The conjugate was diluted to 10 μg ml^{-1} by the addition of HEPES buffer at pH 7.3, and then stored at - 20 °C. The modification of PEI with PEG in the reaction product was determined from proton nuclear magnetic resonance spectrometry (^{1}H-NMR) (400 MHz, Varian) using deuterated water (D_2O) as solvent. The degree of PEG substitution was determined by comparing the integral values obtained from the number of CH_2CH_2O protons of PEG and CH_2CH_2NH protons of PEI [21-23].

2.2.4 PEGylated complexes formation

DNA complexes were formed by addition of cationic polymer (PEI) to plasmid resulting in self-assembled colloidal particles [24]. For PEG-PEIpDNA complexes formation, tetramethylrhodamine-conjugated linear PEI (jetPEI-fluoR 7 mM amine content, Polyplus-Transfection, Illkirch, France) and Ac–PEG-PEI copolymer were added dropwise to plasmid DNA solution. Both polymer and plasmid solutions were diluted in 150 mM NaCl, mixed and incubated for 20 minutes at room temperature to allow complex formation between the positively charged PEI (amine groups) and the negatively charged pDNA (phosphate groups) [25, 26]. Complexes generated using different N (nitrogen) to P (phosphate) ratios (N/P), molar ratio of amine groups of PEI to phosphate groups in pDNA backbone and amounts of PEG molecules, were tested.

2.2.5 Characterization of DNA complexes: size, zeta-potential and bioactivity

In order to optimize the complexes formulation, in terms of best transfection efficiency and lower cytotocixity, PEI/DNA and PEGylated complexes were characterized. The particle size and zeta-potential of the complexes were carried out by dynamic laser light scattering using a Zetasizer Nano-ZS (Malvern

Instruments, Worcestershire, UK). To formed PEI/DNA complexes at different N/P ratios (5, 6 and 10), stock PEI and DNA solutions were prepared and complexes generated by varying the PEI amounts and maintaining constant the pDNA concentration. Then PEGylated complexes were prepared, fixing the N/P ratio at 5 and varying Ac-PEG-PEI copolymer amounts. All measurements were done in triplicate, the mean value was recorded as the average of three different measurements.

Transfection efficiency and cellular cytotoxicity of the DNA complexes, generated according to the different formulations, were tested performing 2D transfection analysis. For transfection experiments, NIH3T3 cells were seeded in 35 mm polystyrene Petri dishes (Corning, Corning, NY, USA) at density of 100,000 cells/dish and incubated at 37 °C and 5 % CO_2, prior to ~80 % confluence, when polymer/DNA complexes containing 3 μg plasmid DNA were added to each well. After 48h, samples were fixed with 4% paraformaldehyde (Sigma Aldrich) for 15 min at RT and stained using 40,6-diamidino-2-phenylindole (DAPI) (Sigma-Aldrich) (maximum excitation at 358 nm; maximum emission at 461 nm) for nuclei detection. The 40,6-diamidino-2-phenylindole stock solution (10 mg ml^{-1} in dimethyl sulfoxide) was diluted in PBS (110^{-4} v/ v), incubated for 10 min at 37 °C, and then rinsed three times with PBS. Analyses of the transfection were carried out using a confocal laser scanning microscope CLSM (Leica TCS SP5 II) equipped with a 25 X objective and a 2P (two-photon)-mode, 700nm laser line emitted by a Coherent Chameleon Ultra Laserand and argon laser lines at wavelengths 488 nm. Image resolution was fixed to 1024 X 1024 pixels. The emitted fluorescence was detected between 420 and 480 nm and between 500 and 530 nm, through different detector channels. Transfection efficiency (number of transfected cells (GFP-expressing cells)/number of cells (DAPI-stained cells)) were quantified through analysis of images using Image J software. Each estimation was repeated in triplicate on different samples. Results were compared by analysis of variance (ANOVA), and a significance level of 95% (P = 0.05) was chosen in all cases.

The biocompatibility of DNA complexes generated according to different formulations was evaluated by colorimetric Alamar blue assay (Life Technologies, Grand Island, NY) according to the manufacturer's procedure [27, 28]. After 24 h of incubation in a humidified atmosphere at 37 °C and 5 % CO_2, NIH3T3 cells seeded onto 24-well plates at an initial density of 25,000 cells/well, were treated with complexes suspensions with different formulations, N/P ratios and Ac-PEG-PEI amounts. The experiments were performed in triplicates and non-trasfected cells were used as a negative control. The metabolic activity of all cell cultures was determined after 1 and 2 days of exposure by using standard Alamar Blue assay. Absorbance of Alamar Blue reagent solution was read at 570 nm and 600 nm by a plate reader (Enspire 2300, Perkin-Elmer). Data represent the cell viability percentage of treated cells normalized to non-treated cells. All experiments were performed in triplicate.

2.2.6 Modification of glass substrates

Glass coverslips of 12 mm Ø (Knittel glass, Germany) were used to covalently bind PEGylated complexes. In order to provide bonding sites (double bonds) for the polyplexes onto the glass surface, 12 mm diameter glass coverslips were treated with two silane solutions. 3-(trimethoxysilyl) propyl methacrylate (TMSPMA, Sigma Aldrich, St. Louis, MO) and 3-aminopropyl triethoxy silane (APTES, Sigma Aldrich, St. Louis, MO) were co-immobilized to the glass coverslips by silane condensation. Prior to modification, the glass coverslips were cleaned carefully by washes with detergent and deionized water, in addition, to remove any surface impurities the slides were immersed in ethanol and ultrasonicated for 10 min and then dried in a nitrogen flow. Next, the substrates were exposed to oxygen plasma excitation for 3 min in a cleaning chamber Plasma Femto (Diener, Böblingen,

Germany) equipped with a 13.56 MHz 100W generator and then treated by immersing with a 0.5 % v/v solution of TMSPMA and APTES in 95% ethanol for 5 minutes. After the silane treatment glass coverslips were extensively rinsed with ethanol to remove residual reagent and dried under a vacuum for 2 h.

2.2.7 Water contact angle

Surface modification of glass slides by silane immobilization was analyzed by water contact angles measurements of water in air at room temperature under static conditions. An Attension Theta optical tensiometer (Biolin Scientific, Stockholm, Sweden) was used to analyze the different wettability of modified substrates in order to verify to the occurrence of chemical modification. An amount of 4 μL droplets of MilliQ water were applied on chemically modified glass surfaces and the pictures was taken with a digital camera. Contact angle was recorded as the angle between the point of contact of the droplet with the solid surface and a tangent with the droplet profile. The contact angle measurement was estimated from a picture and calculated as the mean value of 3 separate measurements, the standard deviation of measurements was < 3°.

2.2.8 Binding of PEGylated complexes to modified glass substrate

Through the activation of glass slides with TMSPMA and APTES silane, methacrylate groups were exposed at surface to allow the photocrosslinking of Ac-PEG-PEIpDNA complexes. In order to induce a covalently bind PEGylated complexes to activated glass slides, modified complexes mixture and 1.5 % (v/v) of a photoinitiator (Irgacure 2959 Ciba, Switzerland) was rapidly exposed to long-wavelength UV light (365 nm, 10mW cm^{-2}, 1 min). After photoreaction between

exposed acryloyl groups, unbound complexes were removed and the substrates were washed twice with 1 X phosphate buffered saline (PBS). The occurrence and distribution of Ac-PEG-PEIpDNA complexes on activated glass substrates were analyzed initially by fluorescence microscopy, through the detection of Cy5 labeled plasmid DNA and rhodamine labeled PEI. Leica TCS SP5 MP, equipped with a 25X water immersion objective was used to acquire images with a resolution of 512 x 512 pixels. Emitted light was detected with two photomultipliers through selected band pass filters. Excitation of rhodamine-labeled PEI, was achieved using the 543 nm excitation line, with the resulting fluorescent wavelengths observed using a 560 - 610 nm band pass filter and excitation of pDNA-Cy5 was achieved with the 633 nm excitation line, with the resulting fluorescence observed using a 650 - 750 nm band pass filter.

2.2.9 Characterization of substrates

To examine the surface modifications and bound complexes morphology atomic force microscopy (AFM) was used. The PEGylated polyplexes was prepared and bind on activated glass slides by photoreaction, as described above. After complexes binding process, surfaces were rinsed with 1 X PBS and with two additional washes in Milli-Q water, to remove any traces of salt on the surface then the samples were allowed to dry in air before imaging. AFM experiments were carried out in “dry” conditions with a BioAFM NanoWizard II (JPK Instruments, Berlin, Germany). Images at 1024 x 1024 pixel resolution were collected at a scan rate of 1 Hz in air at room temperature in contact mode using a silicon nitride tip with a nominal spring constant of 0.01 N m^{-1} (MLCT, Bruker, Billerica, MA, USA). At least three independent imaging scans were obtained for each sample to obtain a representation for each surface.

Substrates and bound complexes morphology was investigated by scanning electron microscopy (SEM), too. Prior to imaging, dried samples were mounted to microscope stub and sputter coated with 5 nm of platinum-palladium under an argon atmosphere using a SEM coating system (Cressingthon, 208 HR, UK). Samples surface morphology was then observed and images were taken using scanning electron microscope (Zeiss, FEG Ultraplus, Germany) with an accelerating voltage of 8 kV and variable magnifications.

2.2.10 Binding efficiency

In order to monitoring the amount of DNA complexes immobilized to the surface after binding reaction, Cy5 labeled plasmid was used. DNA concentration in solution before and following binding reaction was estimated through measures of fluorescence at 633 nm in a multi-well plate spectrofluorometer (Enspire 2300, Perkin Elmer), via a standard curve. Complexes binding efficiency was calculated as the difference between the DNA complexes concentrations, before [C_i] and after [C_f] photoreaction, normalized to initial concentration, in percentage

$$\frac{Ci - Cf}{Ci} * 100$$

The density of the complexes bound to each activated glass slides was established by normalizing the amount of the covalently bound complexes to total area of the substrate.

To evaluate the complexes release from substrates, after efficiency binding tests 400 µl of conditioned medium (cDMEM) were added at the samples and incubated at 37 °C and 5 % CO_2. At scheduled time intervals (24, 48 and 72 h) cDMEM was removed and PEG-PEIpDNA-Cy5 complexes concentration was detected via a standard curve, by measuring the fluorescence at 633 nm, as described above. The

percentage of PEG-PEIpDNA complexes released was calculated with respect to the immobilized amount. Binding and release efficiency results were compared by analysis of variance (ANOVA) with a significance level of 95% (P = 0.05).

2.2.11 Quantification of internalized complexes

To investigate cellular interaction with covalently bound complexes, the amount of DNA complexes internalized by the cells after incubation on modified substrates was evaluated. To this aim, PEGylated complexes, generated using Cy5-labeled plasmid DNA, were covalently bound at activated glass slides, as described above. Immediately following complexes binding, NIH3T3 cells were plated on these modified glass substrates at a density of 7000 cells cm^{-2}, and incubated in culture medium at 37 °C and 5 % CO_2. After scheduled times, cells were roughly rinsed with 1 X PBS, collected via trypsinization, and reseeded on glass dishes (Fluorodish, World Precision Instruments Ltd). After 24h, cells were fixed using 4 % paraformaldehyde (PFA, Sigma Aldrich) for 15 min at RT and observed with a laser scanning confocal microscope (CLSM). An inverted confocal microscope (Leica TCS SP5 II), equipped with a 63X 1.2 NA oil immersion objective was used for the optical sectioning of cells. Excitation of rhodamine-labeled PEI and pDNA-Cy5 was achieved using, respectively, the 543 nm and 633 nm excitation line, while the emitted fluorescence was detected between 550 and 610 nm for Rhodamine-PEI detection and 650 and 750 nm for DNA-Cy5 detection, through different detector channels. Image resolution was fixed to 1024 x 1024 pixels. The intracellular fluorescence of the internalized complexes at different time point was quantified using ImageJ software. Data were reported as the percentage area of the internalized complexes divided by total cellular area. In particular, cell area was evaluated by using plug in Analyze Particles of ImageJ software. At least 15 cells were collected and analyzed for each time point and each substrate.

2.2.12 Complexes intracellular fate_Lysosome co-localization

In order to investigate the intracellular fate of internalized complexes, in particular to localize the polyplexes inside cellular lysosomes, Lysotracker Red DND-99 (Molecular Probes, Invitrogen) was used on non fixed cells following manufacturer's procedure. Briefly, lysosomal compartments were visualized by incubating cells with 0.5 mL Lysotracker Red for 30 min at room temperature prior to confocal microscope acquisition. Co-localization experiments were performed both on cells on complexes modified substrates and on cells detached from substrates and reseeded on fluorodish. The co-localization with PEG-PEIpDNA complexes labeled with Cy5 and subcellular compartments marked with Rhodamine, was assisted by an inverted Leica SP5 confocal microscope. Live cells were imaged through a 63X oil-immersion objective, the resulting image resolution was 1024 X 1024 pixels. Cy5-labeled plasmid DNA was excited by a HeNe laser at 633 nm and fluorescence was observed at 650–750 nm. Lysosomal compartments were visualized through excitation by a HeNe laser at 543 nm and fluorescence was observed at 550–610 nm. Cy5-DNA complexes and lysosomes-Rhod were imaged by confocal microscopy and the colocalization of DNA plasmid in lysosomes was quantified using NIH ImageJ JACoP plugin. By this procedure Pearson's coefficient was calculated in order to estimate a correlation index [29]. At least 17 cells were captured and analyzed per condition.

2.3 Results and Discussions

2.3.1 PEG-PEI conjugate: NMR characterization

The modification of PEI with PEG was assessed by ^{1}H-NMR spectroscopy in D_2O. The degree of PEG substitution of linear PEI (25 kDa) with PEG (3.4 kDa) was

determined by comparing the peaks of CH_2CH_2O protons of PEG (3.58 ppm) and CH_2CH_2NH protons of PEI (2.5 – 3.1 ppm). Results of spectra integration (Figure 1) indicate that the molecular ratio between PEG and PEI in the copolymer is about 60 : 40, therefore, considering the respective molecular weights, in the PEG-PEI conjugate produced each PEI macromolecule was modified with 5 blocks of PEG [30].

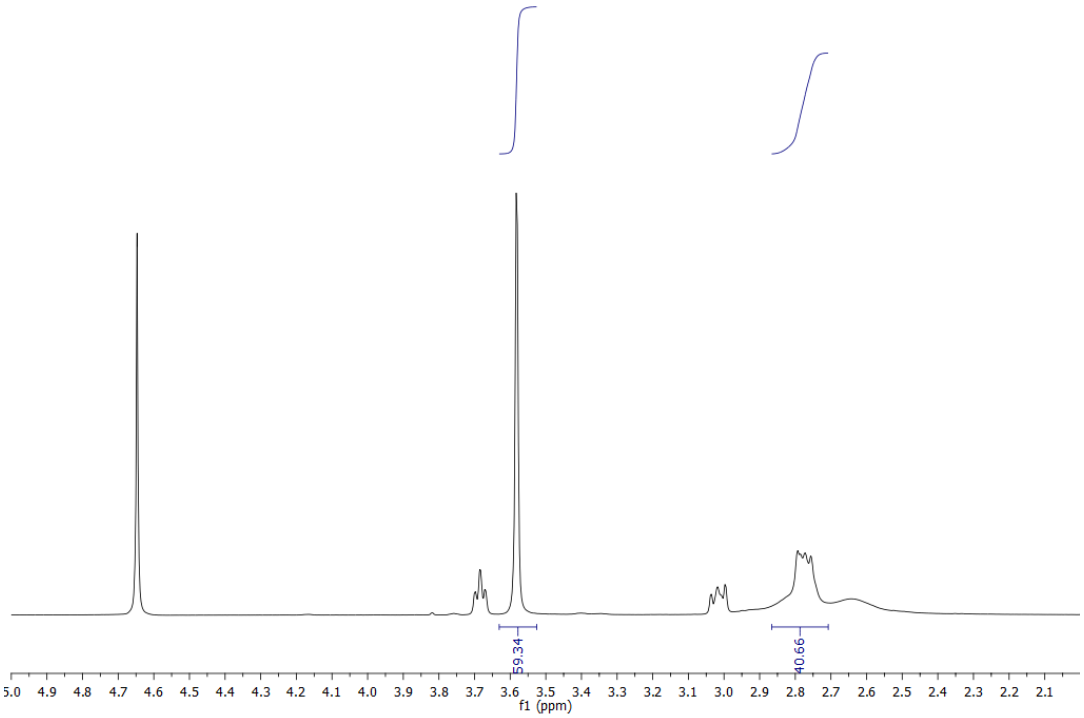

Figure 1 ^{1}HMNR spectrum of PEG-PEI copolymer in D_2O. The peaks at 3.6 ppm was assigned to protons of PEG and the peaks between 2.7 – 2.9 was assigned to protons of PEI. The ratio of PEG/PEI molecules in the copolymer was estimated using integral values

2.3.2 Complexes characterization

To compare different formulations of PEG-PEIpDNA complexes, in terms of N/P ratio and amount of PEG molecules, size, charge, transfection and cellular cytotoxicity of complexes were initially characterized. Particles size and surface charge dictates the interaction of complexes with the cells thereby leading to uptake and efficient transfection [31]. DLS measurements indicate that the complexes diameter, formed at N/P ratio of 5, 6 and 10, ranging from 110 to 150 nm, while zeta potential was about 27 ± 1.3 mV (Table 1). The polydispersity index (PDI) was approximately 0.1, thus indicating narrow size distribution, high uniformity in particle size distribution and overall general homogeneity of the sample. The size and surface charge of the complexes are both important parameters for their interaction and entry into cells [32, 33].

N/P ratio	Size (d.nm)	Z-potential (mV)
5	114 ± 6.3	27 ± 2
6	145 ± 7	28 ± 0,5
10	108 ± 1	25 ± 1

Table 1 Size and zeta potential of polyplexes formulated at N/P ratio of 5, 6, 10.

With particular regards to the surface charge, a balance between the maximal transfection efficiency and the amount of cell death associated with transfection is required [34]. Transfection efficiency and citotoxicity of complexes was evaluated performing 2D transfection analysis on NIH3T3 cells with complexes at N/P ratio of 5, 6 and 10. As shown in fig. 2a, the complexes formed at three different N/P ratios have almost the same transfection efficiency (40%), but the cytotoxicity of

the complexes increase with the N/P ratio (fig. 2b). Taking in account these results, subsequent substrate-mediate delivery experiments were conducted using complexes formed at N/P ratio of 5, that have shown not much affect the cellular viability.

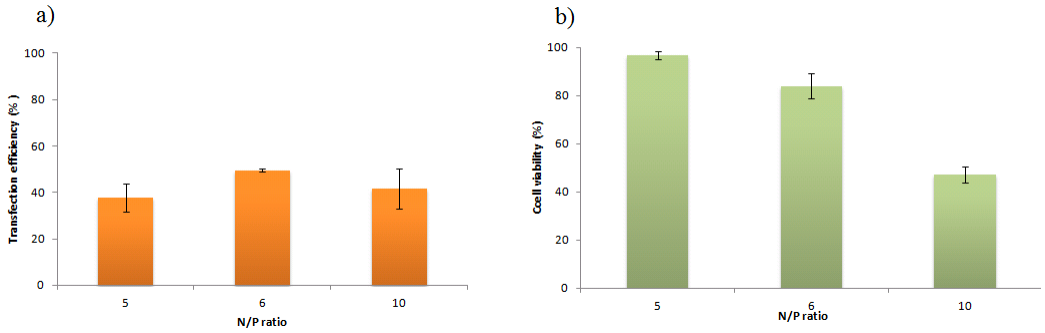

Figure 2 Bioactivity of PEI/DNA complexes generated at N/P ratio of 5, 6 and 10. a) Transfection efficiency, by NIH3T3 cells treated with free polyplexes formed at various N/P ratios and b) cytotoxicity of complexes as function of N/P ratio.

In order to bind gene complexes at a substrates, PEIpDNA complexes were functionalized through the introduction of acryloyl-PEG molecules. Clamme J. P. et al., found that at the molar ratios of PEI nitrogen atoms to DNA phosphate usually used for transfection, ~ 86% of the PEI molecules were in a free form and the PEI/DNA complexes are composed on the average by 3.5 (± 1) DNA plasmids and ~ 30 PEI molecules [35]. Therefore, we have formulated the PEGylated complexes varying the ratio between the amount of linear PEI (jetPEI-fluoR) and Ac-PEG-PEI copolymer, containing about 5 PEG molecules for each PEI macromolecule (NMR results), and, based on a theoretical estimation, calculate the number of PEG molecules for complex. Results of DLS measurements indicate that PEGylation appeared to prevent the size increase (Table 2), rather the diameter of the PEGylated complexes decreases with the increase of the PEG molecules, as

previously reported by most research groups [21]. In general, no remarkable differences in zeta-potential were noted between particles, except for complexes formed with the highest PEG substitution, which demonstrates that PEG molecules mask the positive charge of the PEI molecules, reducing the positive charge exposed at the surface. As expected, the PEGylation leads to a decrease of complexes toxicity [36-38]. The cytotoxicity, calculated as cell viability percentage of treated cells normalized to non-treated cells, has been found to be dependent on the interaction of the PEI/DNA complexes with cell membranes which increases with positive charges exposed on the surface.[39] In particular, the polycationic polymers (like PEI) undergo strong electrostatic interaction with plasma membrane proteins, which can lead to destabilization and ultimately rupture of the cell membrane. Fischer et al. demonstrated that the cytotoxicity of different types of polycationic polymers depend on the number and arrangement of the cationic charges which determines the degree of interaction with the cell membranes and the cells exposed to cationic polymers first show membrane leakage followed by a decrease in the metabolic activity [39]. In our case, the addition of PEG molecules, hiding the positive charge at surface of the PEGylated complexes, cause an increase of the cellular viability and, at same time, a decrease of the cellular uptake and consequently of transfection efficiency (Table 2). Transfection, calculated as the number of transfected cells (GFP-expressing) normalized on total number of cell (DAPI-stained), evaluated through by confocal images was higher with complexes generated with low amount of PEG molecules.

PEG molecules for PEGylated complex	Size (d. nm)	Z-potential (mV)	Transfection efficiency (%)	Cellular viability (%)
5	105 ± 4	23 ± 8	24 ± 3	16 ± 3
10	113 ± 14	27 ± 8	23 ± 5	16 ± 5
30	87 ± 6	27 ± 8	17 ± 4	25 ± 11
75	98 ± 24	25 ±8	18 ± 6	25 ± 7
150	96 ± 5	23 ± 2	2 ± 1	29 ± 10

Table 2 Characterization of PEGylated complexes formed at N/P 5 varying the number of PEG molecules. Results of DLS measurements, transfection efficiency as percentage of NIH3T3 cells expressing GFP and cytotoxicity of PEGylated complexes generated with different amounts of PEG-PEI copolymer.

2.3.3 Characterization of complexes activated substrates

Surface modifications were widely characterized by contact angle, AFM, SEM and confocal microscopy. Fig. 3 depicts a synthesis scheme for preparing the activated substrate. First, the surface of glass slides were activated by oxygen plasma treatment and chemically modified with a silane condensation of Trimethoxysilylpropyl methacrylate (TMSPMA), having a acryloyl group and 3-aminopropyl triethoxysilane (APTES) having an amino group (Fig. 3b). Finally, PEGylated complexes, formed as described in materials and methods section (Fig. 3a), were bound to modified glass substrates via a specific photocrosslink reaction between the respective acryloyl groups (Fig. 3c). To achieve practically sufficient complexes binding (spatial group) APTES silane was co-immobilized with TMSPMA on glass surface [13].

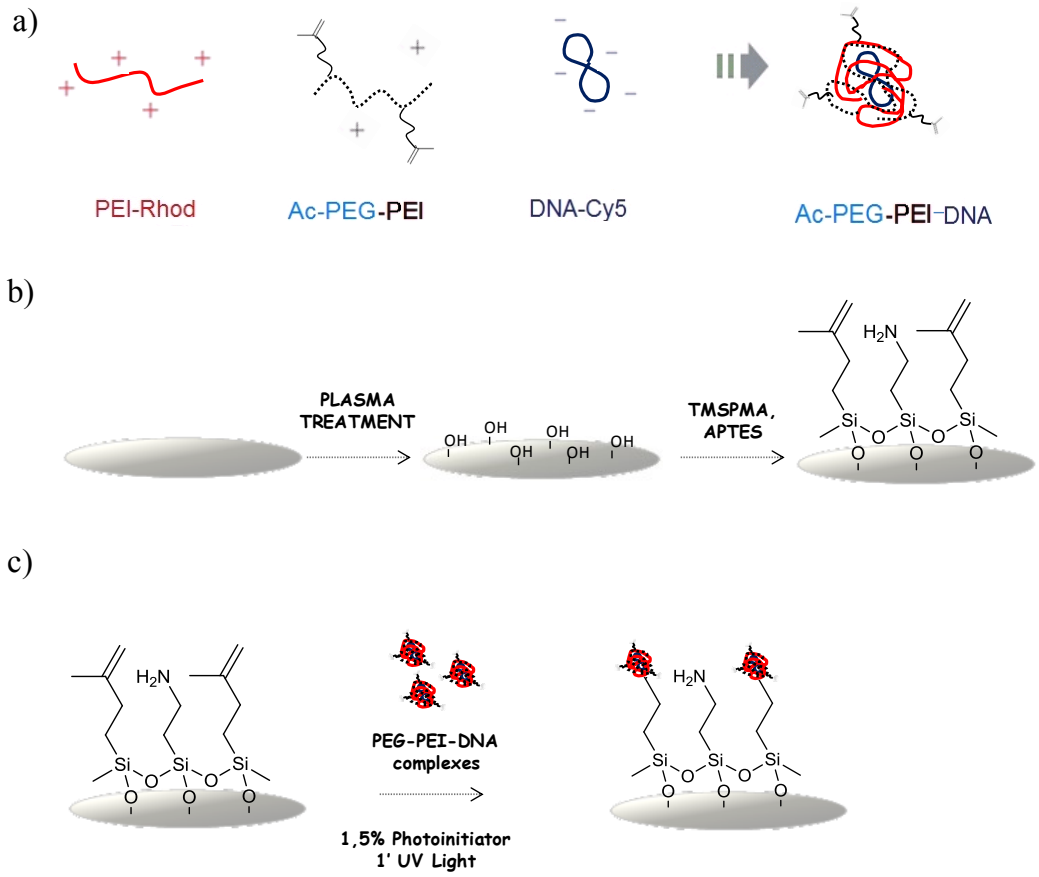

Figure 3 Synthetic scheme of preparation of complexes modified substrates. a) PEGylated complexes formation, b) Chemical activation of glass slides c) Covalent binding of PEGylated complexes with activated glass substrates through a photo-reaction

Chemical modification of the glass surface was confirmed by water contact angle measurements. The quality of the surface treatment was checked by the difference in contact angle of water on silanized and unsilanized glass surface, used as a reference and prepared in exactly the same manner, using equal type of glass, same washing, drying protocol and same type of pre-treatment. Results are shown in Table 3, the TMSPMA and APTES silane coupling treatment decrease the

wettability of the surfaces of glass slides, giving rise to increase in contact angle from 63° ± 1 of the unsilanized glass slides to 76° ± 3 for the glass slides activated with functional groups [40]. Higher the contact angle, higher the hydrophobicity, higher the amount of the present double bonds and consequently higher strength of attachment is expected.

	Glass slides	Silanized glass slides
Contact angle	63° ± 1	76° ± 3

Table 3 Water contact angle measurements on silanized and unsilanized glass slides

Occurrence and persistence of the complexes on the substrates was analyzed, to begin with confocal microscopy due to the presence in the complex of both labeled DNA and PEI. Confocal images show both signals of PEI-Rhod and DNA-Cy5 on substrates, in particular, fig. 4c shown the merge of a and b images and highlight the correspondence of both signals on substrate after binding process.

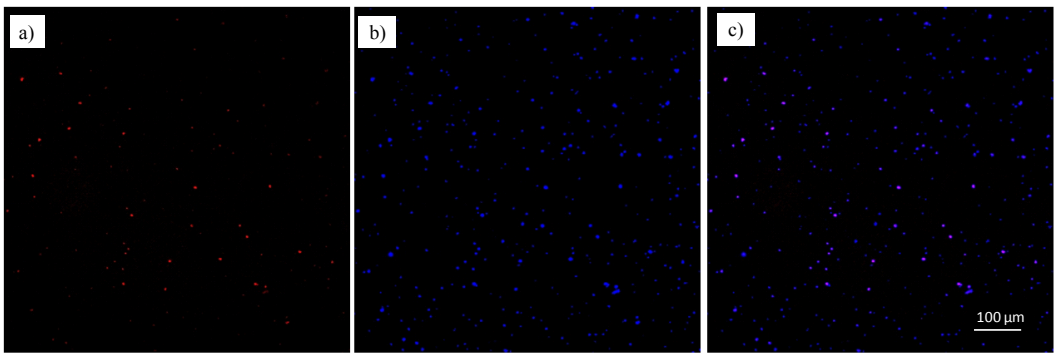

Figure 4 CLSM images of PEGylated complexes tethered to activated glass substrate. (A) PEI-Rhod, (B) DNA-Cy5, (C) merge of A and B images.

Complexes modified glass substrates was characterized, also using atomic force microscopy. AFM has proven to be an excellent tool to image soft biological structures and can be performed after complex deposition on a surface, with high resolution [9]. AFM images were obtained by scanning glass slides with immobilized complexes and representative images (Figure 5) revealed the representative globular morphology of PEGylated complexes on activated substrates [36, 41, 42]. Moreover, the feature height of the bound complexes was similar at the typical diameter of PEGylated complexes, this observation highlight the absence of aggregation of complexes on substrates during the binding process. Previous studies examining complexes using AFM, typically on mica substrates, reported a range of complex morphologies similar to the results presented here. PEGylated PEI–DNA complexes analyzed by AFM had defined, spherical complexes [30–32], with less aggregation and smaller diameters than similar complexes without PEG, but were also demonstrated to be less uniform.

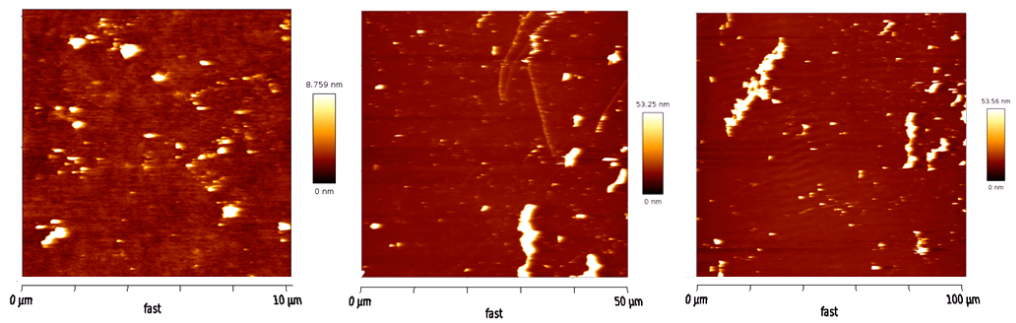

Figure 5 Atomic force microscopy images at different magnifications of PEGylated complexes bound to activated glass substrates

Morphological features of complexes modified substrates by scanning electron microscopy (SEM) clarified the distribution of the complexes on substrates and, in particular, highlighted the circular morphology of the bound complexes (Figure 6).

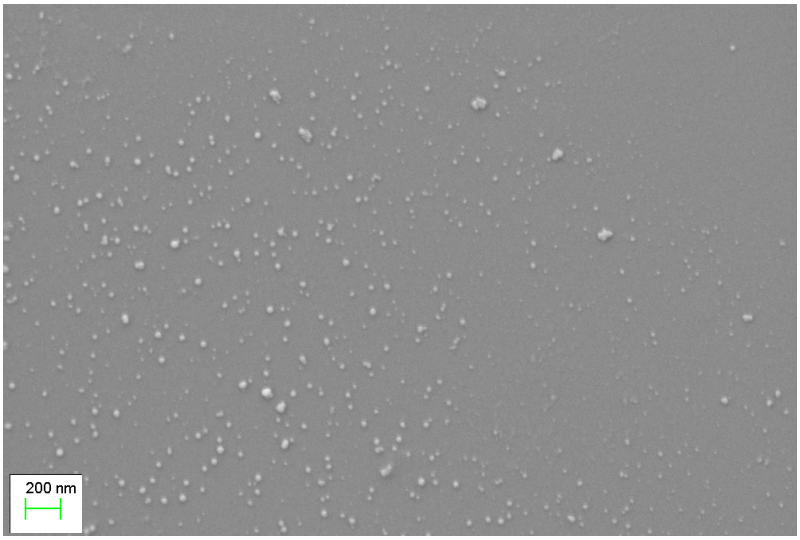

Figure 6 SEM image of PEGylated complexes bound to activated glass substrate

2.3.4 Binding efficiency

Complexes binding efficiency was performed by fluorescence measurements of DNA-Cy5 complexes solutions before and after binding process. For each experimental concentrations tested the percentage of PEGylated complexes bound at activated substrates was about 30 – 40 % concerning the initial amount of DNA complexes put in contact with substrate before photoreaction. Initial DNA concentration and the concentration of the unbound complexes after binding process were showed in the Table 4. Increasing the initial complexes concentration, the efficiency of process decreases, maybe due to aggregation effects between complexes which prevent the surface binding. Therefore, density of DNA

complexes immobilized to the surface ranged from 0.09 μg cm^{-2} to 0.5 μg cm^{-2}, but depends on the concentration with which have prepared the complexes.

C_i (ng/μL)	μg DNA	C_f (ng/μL)	Binding Efficiency (%)	Surface Density (μg/cm^2)
3	0.24	2	34	0.09
6	0.5	4	36	0.18
10	0.84	6	36	0.3
12	1	8	38	0.4
17	1.5	12	30	0.5

Table 4 Binding efficiency of PEGylated complexes to activated glass substrates. C_i complexes concentration initially measured, C_f complexes concentration of unbound complexes after binding process

The quantity of surface associated DNA and the stability of the interaction between the complexes and surface was subsequently measured using CLSM. Analysis of fluorescent images, taken after the initial incubation of labeled complexes on the surface and after each scheduled incubation times, not shown reduction of the fluorescence (Figure 7). These release tests indicate that during the trial time (0 up to 48h), the quantity of surface-associated DNA not change.

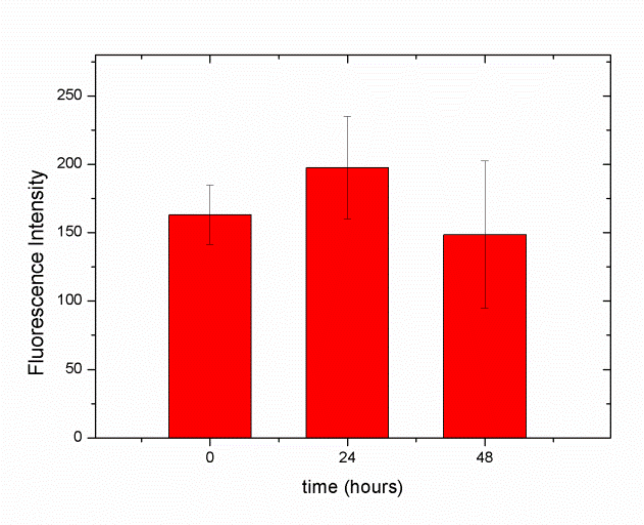

Figure 7 Analysis of fluorescence intensity of DNA-Cy5 complexes immobilized on substrates

2.3.5 Internalized complexes and subcellular distribution

To investigate the cell-substrate interaction, the amount of DNA complexes internalized by the cells after incubation on this complexes modified substrates was evaluated. Quantification of the internalized complexes from cells seeded on modified substrates was assessed using Cy5-labeled plasmid DNA to formed PEGylated complexes. To distinguish easily DNA-Cy5 complexes inside or outside the cells present on substrate, after 24h culture on bound complexes, NIH3T3 cells were detached from this functionalized substrates and reseeded on inert dish. Fluorescence of intracellular complexes was monitored the in time by confocal microscope acquisition and the percentage area of the cells occupy by internalized complexes was calculate through the images elaboration using Image J software. Results are shown in figure 8, comparing samples and controls, the complexes percentage internalized from surface are much lower than bolus delivery. Nearly all

cells on surfaces with immobilized complexes had internalized DNA, but not statistical difference of the number of complexes internalized in time was detected. In particular, the percentage area of transfected cells occupied by complexes, obtained only with bolus delivery, was approximately twenty time higher of complexes internalized with substrate-mediated delivery. Maybe, there is an hypothetical minimum threshold of internalized complexes that provides the transfection. Monitoring the internalization process, the percentage of the internalized complexes from substrates not change over time, likewise for the complexes internalized with bolus delivery. These results indicate a low internalization efficiency probably due to a low density of complexes immobilized to the substrate for reverse transfection.

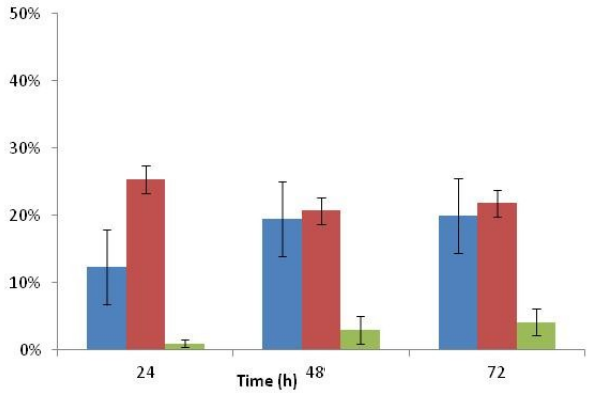

Figure 8 Quantification of internalized complexes by the cells seeded on modified substrates. Percentage cellular area occupied by internalized complexes during time. Blue bar for bolus delivered complexes, red bar for cells expressing GFP and green bar for substrate-mediated delivered complexes

To investigate the intracellular fate of the internalized complexes, subcellular distribution was subsequently characterized. In particular the co-localization of DNA complexes with lysosomes compartments was analyzed by confocal

microscopy, and quantified using NIH ImageJ software. For substrate-mediated delivery, the mean percentages of lysosomal DNA is more relevant than bolus delivery. In the table 5 were reported Pearson's coefficients obtained by ImageJ JACoP plugin for the different delivery systems in order to evaluate a correlation index (< 0.5 low correlation index, >0.5 high correlation index) . The values of Pearson's coefficients highlight the difference between complexes delivered through bolus and substrate-mediated delivery, and suggests that the internalization pathway or cellular trafficking can differ for polyplexes delivered from the surface relative to bolus.

	Pearson's coefficient
Sample: cells on substrate	0,57 ± 0,11
Detached & reseeded cells	0,66 ± 0,1
Ctrl_free complexes	0,37 ± 0,1

Table 5 Pearson's coefficient values.

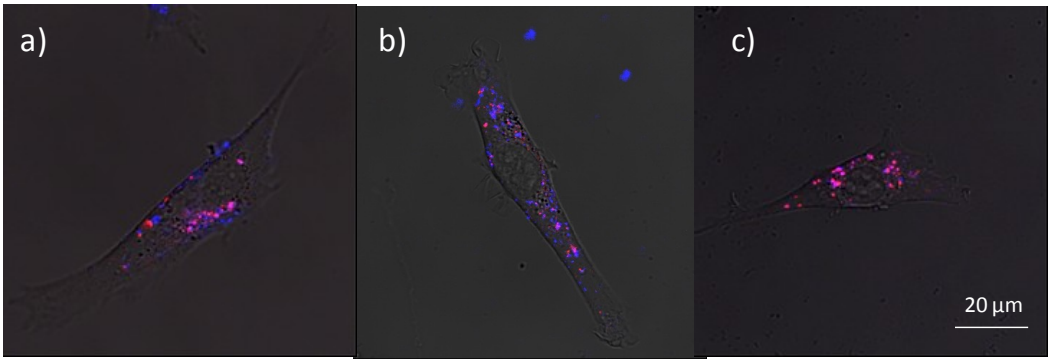

Figure 9 CLSM images of co-localization of Cy5 labeled plasmid with lysosome a) cells on dishes with free complexes b)cells on bounded complexes c) cells detached from modified substrate and reseeded on inert dish. blue spots indicate Cy5-plasmid, red spots indicate lysosome

2.4 References

1. Schena, M., et al., *Microarrays: biotechnology's discovery platform for functional genomics.* Trends Biotechnol, 1998. **16**(7): p. 301-6.
2. Silverman, L., R. Campbell, and J.R. Broach, *New assay technologies for high-throughput screening.* Curr Opin Chem Biol, 1998. **2**(3): p. 397-403.
3. Bailey, S.N., R.Z. Wu, and D.M. Sabatini, *Applications of transfected cell microarrays in high-throughput drug discovery.* Drug Discov Today, 2002. **7**(18 Suppl): p. S113-8.
4. King, K.R., et al., *A high-throughput microfluidic real-time gene expression living cell array.* Lab Chip, 2007. **7**(1): p. 77-85.
5. Ziauddin, J. and D.M. Sabatini, *Microarrays of cells expressing defined cDNAs.* Nature, 2001. **411**(6833): p. 107-10.
6. Bonadio, J., *Tissue engineering via local gene delivery:: Update and future prospects for enhancing the technology.* Advanced drug delivery reviews, 2000. **44**(2): p. 185-194.
7. Jang, J.-H., D.V. Schaffer, and L.D. Shea, *Engineering biomaterial systems to enhance viral vector gene delivery.* Molecular Therapy, 2011. **19**(8): p. 1407-1415.
8. Pannier, A.K. and L.D. Shea, *Controlled release systems for DNA delivery.* Mol Ther, 2004. **10**(1): p. 19-26.
9. Pannier, A.K., J.A. Wieland, and L.D. Shea, *Surface polyethylene glycol enhances substrate-mediated gene delivery by nonspecifically immobilized complexes.* Acta Biomater, 2008. **4**(1): p. 26-39.
10. Adler, A.F. and K.W. Leong, *Emerging links between surface nanotechnology and endocytosis: impact on nonviral gene delivery.* Nano Today, 2010. **5**(6): p. 553-569.

11. Bengali, Z., et al., *Gene delivery through cell culture substrate adsorbed DNA complexes.* Biotechnol Bioeng, 2005. **90**(3): p. 290-302.
12. Segura, T., M.J. Volk, and L.D. Shea, *Substrate-mediated DNA delivery: role of the cationic polymer structure and extent of modification.* J Control Release, 2003. **93**(1): p. 69-84.
13. Akimoto, A.M., T. Takarada, and M. Maeda, *Preparation of cell-culturing glass surfaces that release branched polyethyleneimine triggered by thiol-disulfide exchange.* Colloids Surf B Biointerfaces, 2013. **103**: p. 360-5.
14. Moy, V.T., E.L. Florin, and H.E. Gaub, *Intermolecular forces and energies between ligands and receptors.* Science, 1994. **266**(5183): p. 257-9.
15. Alferiev, I.S., et al., *Surface heparinization of polyurethane via bromoalkylation of hard segment nitrogens.* Biomacromolecules, 2006. **7**(1): p. 317-22.
16. Harris, J.M., *Poly (ethylene glycol) chemistry: biotechnical and biomedical applications*. 1992: Springer Science & Business Media.
17. Goddard, J.M. and J. Hotchkiss, *Polymer surface modification for the attachment of bioactive compounds.* Progress in polymer science, 2007. **32**(7): p. 698-725.
18. Vidic, J., A. Podgornik, and A. Strancar, *Effect of the glass surface modification on the strength of methacrylate monolith attachment.* J Chromatogr A, 2005. **1065**(1): p. 51-8.
19. Plueddemann, E.P., *Silane coupling agents*. 1982: Springer Science & Business Media.
20. Ludtke, J.J., M.G. Sebestyen, and J.A. Wolff, *The effect of cell division on the cellular dynamics of microinjected DNA and dextran.* Mol Ther, 2002. **5**(5 Pt 1): p. 579-88.
21. Fitzsimmons, R.E. and H. Uludag, *Specific effects of PEGylation on gene delivery efficacy of polyethylenimine: interplay between PEG substitution and N/P ratio.* Acta Biomater, 2012. **8**(11): p. 3941-55.

22. Kursa, M., et al., *Novel shielded transferrin-polyethylene glycol-polyethylenimine/DNA complexes for systemic tumor-targeted gene transfer.* Bioconjug Chem, 2003. **14**(1): p. 222-31.
23. Nguyen, H.K., et al., *Evaluation of polyether-polyethyleneimine graft copolymers as gene transfer agents.* Gene Ther, 2000. **7**(2): p. 126-38.
24. Boussif, O., et al., *A versatile vector for gene and oligonucleotide transfer into cells in culture and in vivo: polyethylenimine.* Proc Natl Acad Sci U S A, 1995. **92**(16): p. 7297-301.
25. Dunlap, D.D., et al., *Nanoscopic structure of DNA condensed for gene delivery.* Nucleic Acids Res, 1997. **25**(15): p. 3095-101.
26. Minagawa, K., et al., *Direct observation of the biphasic conformational change of DNA induced by cationic polymers.* FEBS Lett, 1991. **295**(1-3): p. 67-9.
27. Nakayama, G.R., et al., *Assessment of the Alamar Blue assay for cellular growth and viability in vitro.* J Immunol Methods, 1997. **204**(2): p. 205-8.
28. Nociari, M.M., et al., *A novel one-step, highly sensitive fluorometric assay to evaluate cell-mediated cytotoxicity.* J Immunol Methods, 1998. **213**(2): p. 157-67.
29. Costes, S.V., et al., *Automatic and quantitative measurement of protein-protein colocalization in live cells.* Biophysical journal, 2004. **86**(6): p. 3993-4003.
30. Tang, G.P., et al., *Polyethylene glycol modified polyethylenimine for improved CNS gene transfer: effects of PEGylation extent.* Biomaterials, 2003. **24**(13): p. 2351-62.
31. Nimesh, S., et al., *Improved transfection efficiency of chitosan-DNA complexes employing reverse transfection.* Journal of Applied Polymer Science, 2012. **124**(3): p. 1771-1777.
32. Oku, N., et al., *The fusogenic effect of synthetic polycations on negatively charged lipid bilayers.* J Biochem, 1986. **100**(4): p. 935-44.

33. Bettinger, T., J.S. Remy, and P. Erbacher, *Size reduction of galactosylated PEI/DNA complexes improves lectin-mediated gene transfer into hepatocytes.* Bioconjug Chem, 1999. **10**(4): p. 558-61.

34. Plank, C., et al., *Activation of the complement system by synthetic DNA complexes: a potential barrier for intravenous gene delivery.* Hum Gene Ther, 1996. **7**(12): p. 1437-46.

35. Clamme, J.P., J. Azoulay, and Y. Mely, *Monitoring of the formation and dissociation of polyethylenimine/DNA complexes by two photon fluorescence correlation spectroscopy.* Biophys J, 2003. **84**(3): p. 1960-8.

36. Petersen, H., et al., *Polyethylenimine-graft-poly(ethylene glycol) copolymers: influence of copolymer block structure on DNA complexation and biological activities as gene delivery system.* Bioconjug Chem, 2002. **13**(4): p. 845-54.

37. Malek, A., F. Czubayko, and A. Aigner, *PEG grafting of polyethylenimine (PEI) exerts different effects on DNA transfection and siRNA-induced gene targeting efficacy.* J Drug Target, 2008. **16**(2): p. 124-39.

38. Sung, S.J., et al., *Effect of polyethylene glycol on gene delivery of polyethylenimine.* Biol Pharm Bull, 2003. **26**(4): p. 492-500.

39. Fischer, D., et al., *In vitro cytotoxicity testing of polycations: influence of polymer structure on cell viability and hemolysis.* Biomaterials, 2003. **24**(7): p. 1121-31.

40. Kurth, D.G. and T. Bein, *Monomolecular layers and thin films of silane coupling agents by vapor-phase adsorption on oxidized aluminum.* The Journal of Physical Chemistry, 1992. **96**(16): p. 6707-6712.

41. Merdan, T., et al., *PEGylation of poly(ethylene imine) affects stability of complexes with plasmid DNA under in vivo conditions in a dose-dependent manner after intravenous injection into mice.* Bioconjug Chem, 2005. **16**(4): p. 785-92.

42. Mao, S., et al., *Influence of polyethylene glycol chain length on the physicochemical and biological properties of poly(ethylene imine)-graft-poly(ethylene glycol) block copolymer/SiRNA polyplexes.* Bioconjug Chem, 2006. **17**(5): p. 1209-18.

Chapter 3

Reverse transfection by PEGylated complexes adsorbed to a solid substrate: role of surface density

3.1 Introduction

The potential applications of gene transfer cover both basic and applied sciences and relate to functional genomics, gene therapy, and tissue engineering. *In vivo* gene delivery of naked DNA requires that the plasmid must overcome several intra and extracellular barriers that limit the efficiency of gene transfer. The complexation of plasmid DNA with viral or non viral vectors, supports the cellular internalization and transfection, but are not always assures the correct efficiency and duration of gene expression. Gene vectors, can facilitate intracellular trafficking, which includes endosomal escape, cytoplasmic transport, and nuclear entry, while also dissociating from the DNA to allow expression [1, 2]. Non-viral vectors, in particular, are safer and easier to prepare than viral vectors, but typically have lower efficiency and shorter duration of gene expression [3]. Relative to more traditional delivery methods, controlled delivery systems have the potential to overcome extracellular barriers, as well as enhance gene delivery [4]. These different approaches deliver vectors according to two main mechanisms: (i) polymeric release, in which the DNA is released from the polymer, or (ii) substrate-mediated delivery, in which DNA is retained at the surface. While forward transfection adds gene particles to previously seeded cells, substrate-mediated delivery, also termed reverse transfection or solid-phase tranfection, immobilizes the DNA to a substrate that supports cell adhesion, placing the vector directly in the cellular microenvironment, which has been shown to enhance gene delivery [5]. Cells cultured on the substrate can internalize the DNA either directly from the surface, or after release from the surface. The retention or release of DNA from surface can be dictated by the strength and specificity of the molecular interactions between the vector and substrate. Specific interactions can be introduced through complementary functional groups on the vector and surface, such as antigen–antibody or biotin–avidin [6, 7]. Viral vectors have been designed

to specifically interact with biomaterials through the use of antibodies or covalent coupling to allow for site-specific gene delivery [8]. While poly(L-lysine) (PLL) and polyethylenimine (PEI), modified with biotin residues, have been complexed with DNA and bound to a neutravidin substrate [9]. The increase in the number of biotin groups per complex leads to increased binding, however, if the association of complexes with a substrate is too tight, endocytic uptake and transfection can suffer [10]. Alternatively, nonspecific mechanisms, including hydrophobic, electrostatic, and van der Waals interactions, can be used to bind viral and nonviral vectors to a substrate. These interactions, mainly, occur by adsorption of gene vectors to a polymeric systems, which have been shown to enhance the gene expression and cellular viability [4]. However nonspecific binding depends upon the molecular composition of the vector (e.g., lipid, polymer, protein) and the relative quantity of each (e.g., N/P) [4]. Although the immobilization of vectors provides many advantages concern to transfection efficiency, a correct balance between the binding of the vector to the substrate and the ability to release the vehicle for cellular uptake is required. The effective affinity of the vector for the substrate may also be influenced by environmental conditions (e.g., ionic strength, pH), binding-induced conformational changes, or vector unpacking. Another limiting factor in nonviral gene delivery is the concentration of DNA at the cell surface [5]. Inefficient transfection of conventional bolus delivery systems is due to mass transport issues, indeed, the delivery process of the complexes to the cell surface is typically a diffusion-limited process, whereas reverse transfection can pre-load complexes at high levels onto the cell—substrate interface [10]. Increasing the amount of DNA immobilized at surface during reverse transfection increases expression levels [11]. On the other hand, aggregation effects due to high density of the complexes on substrate, may lead to weaker binding and consequent release from substrate. The chemistry of substrate also can affect the immobilization and expression of non viral vectors. Inclusion of PEG-like moieties, for instance, can increase the transfection efficiency of PEI polyplexes adsorbed to monolayers of

carboxylic endgroups [12]. Nevertheless, this increase cannot be attributed to an increase in complex binding or release, but the size and shape of adsorbed complexes is markedly affected.

In this study PEG molecules were added to PEI/DNA complexes then adsorbed to a glass substrates. Morphology of PEGylated complexes modified substrate, cellular uptake profile and reverse transfection were characterized. In particular, substrate adsorption and transfection efficiency have been tested varying the amount of DNA complexes aspecifically immobilized at surface. To maximize cellular transfection, the density of the DNA complexes on substrate has to be sufficient to support gene expression yet not so excessive as to compromise cellular viability. Manipulating the concentration of the complexes on substrate has been possible to modulate the transfection efficiency, on the other hand the cellular uptake profile indicates that substrate release probably affect cellular transfection.

3.2 Materials and Methods

3.2.1 Materials

The reporter plasmid encoding for enhanced green fluorescent protein (EGFP) driven by a cytomegalovirus (CMV) promoter was amplified in *Escherichia coli*, extracted and purified from bacteria culture using Qiagen plasmid kit (Santa Clara, CA). Tetramethylrhodamine-conjugated linear PEI (JetPEI-Rhod) was purchased from Polyplus-transfection SA (7mM ammine content, Illkirch, France). Linear PEI 25 kDa purchased from Polysciences (Warrington, PA) was conjugated to acryloyl-PEG-N-hydroxysuccinimmide (Ac-PEG-NHS, 3.4 kDa, Creative PEG Works, Winston-Salem, NC). Label IT® Tracker™ Intracellular Nucleic Acid

Localization Kit was purchased from Mirus Bio (Madison, WI, USA). LysoTracker Red DND-99 was purchased from Molecular Probes (Invitrogen, Oregon, USA).

3.2.2 Cell culture

Transfection studies were performed with NIH/3T3 mouse fibroblasts cultured in humidified 5 % CO_2 atmosphere at 37 °C in Dulbecco's modified Eagle's medium with 4.5 g L^{-1} glucose (DMEM) (Gibco) supplemented with 10 % (*v/v*) bovine calf serum (BCS) (Gibco), 4 mM glutamine, 100 U mL^{-1} penicillin and 0.1 mg mL^{-1} streptomycin in 100 mm diameter cell culture dish (Corning Incorporated, Corning, NY). The cells were routinely splitted using 0.25% trypsin (Trypsin-EDTA, Invitrogen) following standard protocols.

3.2.3 Amplification and purification of plasmid DNA

Plasmid DNA, p^{CMV}EGFP, containing a reporter gene encoding for enhanced green fluorescent protein (EGFP) was used for transfection studies. The chemically competent DH5α^{TM} bacterial strain (*Escherichia coli* species) was transformed with p^{CMV}EGFP using heat shock method. The pDNA in the transformed culture was then expanded in *E. coli* in Lennox L Broth (LB Broth) supplemented with 100 mg L^{-1} ampicillin overnight at 37 °C in an incubator shaker at 300 rpm. Plasmid DNA was extracted and purified from bacterial culture using a Qiagen kit (Santa Clara, CA) according to the manufacturer's specifications. The purity was confirmed by 1% agarose gel electrophoresis follows by ethidium bromide staining and the concentration of pDNA solution was determined using a NanoDrop 2000 UV-Vis Spectrophotometer (Thermo Scientific, Wilmington, DE) by measuring the absorbance at 260nm.

3.2.4 Covalent labeling of plasmid DNA

Plasmid DNA was covalently labeled with the cyanine dye Cy5 using Label IT® Tracker™ Intracellular Nucleic Acid Localization Kit (Mirus Bio, Madison, WI, USA). The labeling reaction was carried out at a ratio of 0.5 µl of Label IT® Tracker™ reagent to 1 µg of plasmid DNA for 1 h at 37 °C followed by an ethanol precipitation step to remove unbound Label IT reagent as recommended by the manufacturer's instructors [13]. The labeled DNA was recovered by centrifugation at 13,000 rpm for 10 minutes. The pellet was washed with 70% ethanol and resuspended in H_2O. (3.6ppm) with (The purity of labeled plasmid was confirmed by measuring the ratio of absorbance at 260 nm and 280nm (A_{260nm}/A_{280nm}) at NanoDrop 2000 UV-Vis Spectrophotometer.

3.2.5 Synthesis of PEG-PEI copolymer

Linear Polyethylenimine (L-PEI) 25kDa (Polysciences, Warrington, PA) was conjugated to acryloyl-PEG-N-hydroxysuccinimmide (Ac-PEG-NHS, 3400 Da, Creative PEG Works, Wiston-Salem, NC, USA). Conjugation was carried out in solution by mixing a solution of PEI HCl 0.7 µmol dissolved in 1 mL of 20 mM HEPES, at pH 7.1, with 50 equiv of acryloyl-PEG-NHS dissolved in 0.7 mL of DMSO for 1h. After the incubation, Ac-PEG-PEI copolymer was dialyzed and lyophilized before use. The modification of PEI with PEG in the reaction product was determined by proton nuclear magnetic resonance spectrometry (^{1}H-NMR) (400 MHz, Varian) using deuterated water (D_2O) as solvent, the degree of PEG substitution was calculated by comparing the peaks of CH_2CH_2O (3.58 ppm) of PEG with CH_2CH_2NH (~ 2.5 – 3.1 ppm) of PEI [14, 15].

3.2.6 Complexes formation and characterization

Plasmid DNA (p^{CMV}EGFP) encoding for enhanced green fluorescent protein (EGFP), purified from bacteria culture using Qiagen exaction kit (Santa Clara, CA) was complexed with tetramethylrhodamine-conjugated linear PEI (JetPEI-fluoR 7mM amine content, Polyplus-transfection, Illkirch, France) (maximum excitation at 555 nm; maximum emission at 580 nm) and PEG-PEI copolymer (0.01 mg mL^{-1} in HEPES 100 mM) at final N/P ratio of 5. Both plasmid DNA (3μg) and PEI (6 μl jetPEI-R and 3 μl Ac-PEG-PEI) were diluted in 100 μl of 150 mM NaCl, rapidly mixed by pipetting up and down and adding PEI solution to DNA solution [16]. Polyplexes were allowed to stand for 20 min at RT before use.

Measurements of size and ʒ-potential of DNA complexes were performed using a Zetasizer Nano ZS (Malvern Instruments, Worcestershire, UK). PEG-PEIpDNA complexes at N/P ratio of 5 were generated in deionized water to a DNA concentration of 27 μg mL^{-1} and subsequently diluted to a final concentration of 6 μg mL^{-1}, before the measurement. Zeta-potential was measured electrophoretically by the laser scattering technique using folded capillary cells. All measurements were done in triplicate, the mean value was recorded as the average of three different runs.

3.2.7 Complexes adsorption on glass substrates

After preparation PEGylated complexes were adsorbed by 2 h incubation on glass substrates. In order to evaluate the adsorption efficiency by fluorescence measures, plasmid DNA was labeled with Cy5 dye using Label IT® Kit (Mirus Bio) and DNA concentration of PEG-PEIpDNA complexes solutions was monitored before and after adsorption. Different polyplexes solutions at known DNA-Cy5 concentration (6 – 12 – 19 – 24 μg mL^{-1}) were adsorbed on Φ 12 mm glass slides

(Knittel glass, Germany) for 2 h at room temperature. After this incubation time, DNA-Cy5 concentration of the unbound complexes was detected via a standard curve, by measuring the fluorescence of DNA-Cy5 at 633 nm in a multi-well plate spectrofluorometer (Enspire 2300, Perkin Elmer, USA). The complexes adsorption efficiency was expressed as the difference between the complexes concentration initially incubated on the substrate and the concentration of unbound complexes after the incubation time, normalized on initial concentration, in percentage

$$\frac{[Ci] - [Cf]}{[Ci]} * 100$$

Where $[C_i]$ and $[C_f]$ are the initial and final concentrations of complexes solutions measured before and after adsorption process, respectively. The experiments were repeated in triplicate with different samples, for each DNA concentration tested. The density of DNA complexes immobilized to each sample was determined by normalizing the amount bound to area of substrate.

3.2.8 Characterization of complexes modified substrates: AFM – SEM.

Morphology and surface distribution of adsorbed complexes were scanned by atomic force and electron microscopy (AFM - SEM). Polyplexes was prepared and immobilized on glass substrates as described above. Two kind of samples were prepared with different amount of PEGylated complexes immobilized (1 – 2 μg DNA), after adsorption process, complexes modified substrates were rinsed with Milli-Q water to remove any traces of salt on surface, then the samples were allowed to dry in air. AFM experiments were carried out in "dry" conditions with a BioAFM NanoWizard II (JPK Instruments, Berlin, Germany) with a MLCT (Bruker, Billerica, MA, USA) silicon tip in contact mode at a scan rate of 1 Hz with a spring constant around 0.01 N m^{-1}. Multiple measurements at different magnifications were taken in air, at room temperature, at 1240 x 1240 pixels resolution to obtain a good representation of the whole surface. Complexes

modified substrates were processed for visualization also by scanning electron microscopy (SEM). After complexes immobilization, samples were mounted on SEM stubs and coated using a SEM coating system (Cressingthon, 208 HR, UK) with 5 nm of platinum-palladium under an argon atmosphere, and analyzed by SEM (Zeiss, FEG Ultraplus, Germany) at an accelerating voltage of 8.7 kV, and at variable magnifications.

3.2.9 Substrate-mediated transfection studies

For substrate-mediated transfection studies, PEG-PEIpDNA complexes (1ug - 2ug DNA) generated at N/P ratio of 5 were adsorbed at the surface of glass substrates (Φ 12 mm Fluorodish, World Precision Instruments Ltd). Immediately following complexes immobilization, NIH3T3 cells were plated on complexes modified substrates at a density of 7000 cells cm^{-2} and incubated in culture medium at 37 °C and 5% CO_2 until transfection was analyzed. The efficiency of gene transfer was monitored by expression of reporter transgene encoding for green fluorescent protein. Control studies were performed through bolus delivery of PEGylated complexes with NIH3T3 cells plated on Φ 12 mm fluorodish at density of 7000 cells cm^{-2}. Day after, the same the amount of DNA immobilized to the substrates was added free to the previously seeded cells for bolus delivery. Usually, the complexes deliver by bolus method were generated according to the same quantity of immobilized DNA on substrate for reverse transfection but in 10% of the volume [16]. Transfection was characterized through confocal laser scanning microscopy (CLSM). After scheduled incubation times, samples were fixed with 4% paraformaldehyde (Sigma Aldrich, USA) for 20 min and stained with 40,6-diamidino-2-phenylindole (DAPI) (Sigma-Aldrich) (maximum excitation at 358 nm; maximum emission at 461 nm) for nucleus detection. Transfection analyses were carried out using a laser scanning confocal microscope (Leica TCS SP5)

equipped with a 25 X objective. Image resolution was fixed to 1024 X 1024 pixels. Samples were detect by 2P (two-photon)-mode, 700nm laser line emitted by a Coherent Chameleon Ultra Laser and an argon laser, at wavelengths of 488 nm. The emitted fluorescence was detected between 420 and 480 nm and between 500 and 530 nm, through different detector channels. The percentage of transfected cells was calculated as the ratio of the transfected cells, GFP-expressing cells, and total cell number, DAPI-stained cells, quantified by analysis of images using Image J software. All experimental conditions were performed in triplicate.

3.2.10 Cellular internalization of DNA complexes

To evaluated the amount of DNA complexes internalized by the cells after incubation on modified substrates, fluorescence of intracellular complexes was monitored by confocal laser scanning microscopy (CLSM). Samples were prepared as described above, immobilizing Cy5 labeled polyplexes at glass substrates and seeding NIH3T3 cells after adsorption process. Cells were harvested 24, 48, 72 h after exposure to complexes modified substrates and reseeded on cell culture dishes (Fluorodish), after 24 h culture samples were fixed using 4% paraformaldehyde (Sigma Aldrich) for 20 min at RT. To detect fluorescence intracellular, an inverted confocal microscope Leica TCS SP5 II equipped with a 63X/1.4 NA oil objective was used. Excitation of rhodamine-labeled PEI and Cy5-labeled pDNA was achieved using, respectively, the 543 nm and 633 nm excitation line, while the emitted fluorescence was detected, between 550 and 610 nm for rhodamine detection and between 650 and 750 nm for Cy5 detection. Image resolution was fixed to 1024 x 1024 pixels. The fluorescence of the PEGylated complexes internalized by the cells at different time points was quantified using Image J software. Data were reported as the percentage of cellular area (A_{cell})occupied by the internalized fluorescent complexes (A_{comp})

$$\frac{Acomp}{Acell} * 100.$$

At least 15 cells were collected and analysed for each time point and each substrate.

3.2.11 Lysosome co-localization

To monitoring the amount of the internalized complexes co-localized with lysosomal compartments, cells on substrates and harvested from complexes modified substrates were incubated with 0.5 mL Lysotracker Red DND-99 (Molecular Probes, Invitrogen) for 30 min at room temperature prior to confocal acquisition. Image were acquired with inverted SP5 Leica microscope equipped with a 63X oil immersion objective a resolution of 1024 x 1024 pixels. Sequential scanning was used to control for spectral overlap between fluorophores, with 8 line averaging to improve signal-to-noise ratios. Intracellular DNA-Cy5 complexes were visualized by excitation by a HeNe laser at 633 nm and fluorescence was observed at 650–750 nm, while lysosome were visualized by excitation by a HeNe laser at 543 nm and fluorescence was observed at 550–610 nm. Quantification of DNA complex localization within lysosomal compartments was estimated by calculation of Pearson's coefficient using NIH ImageJ software JACoP plug-in [17].

3.2.12 Statistical analysis

All quantitative date were reported as means ± standard deviation (SD). Statistical analyses were performed using a one-way analysis of variance (ANOVA). Results

were compared by analysis of variance (ANOVA) and a p-value < 0.05 was considered statistically significant.

3.3 Results and Discussions

3.3.1 PEG-PEI conjugate characterization

PEG-PEI conjugation was characterized by ^{1}H-NMR spectroscopy in D_2O. ^{1}H-NMR spectra integration (Fig. 1) indicates that in the PEG-PEI copolymer there are about 1.5 PEG molecules for each PEI macromolecule [18]

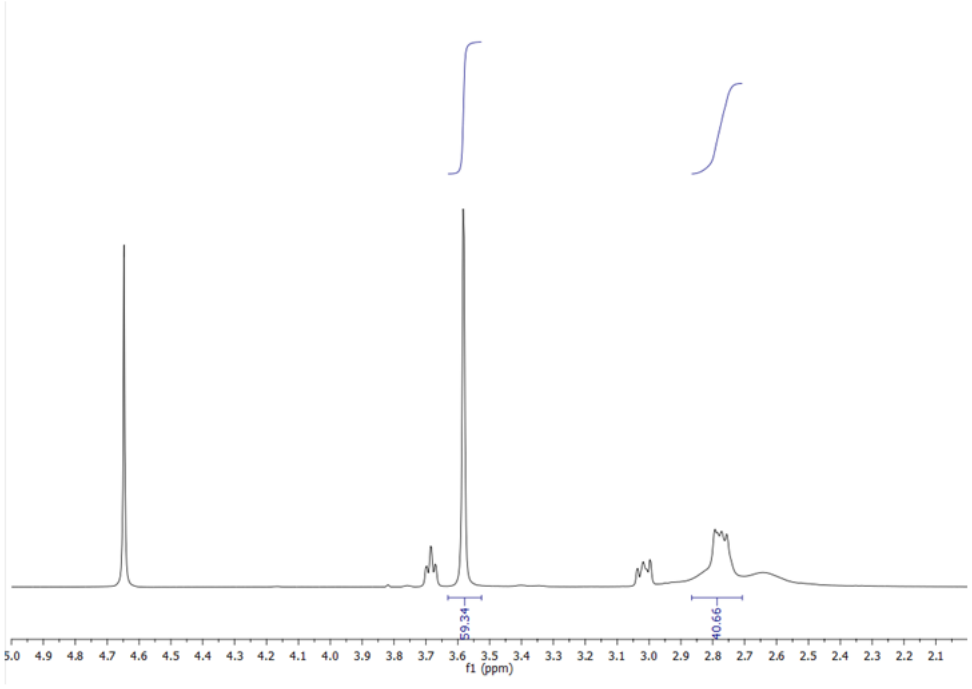

Figure 1 ^{1}HNMR spectrum of PEG-PEI copolymer in D_2O. PEG substitution was determined by comparing the peaks of CH_2CH_2O (3.6 ppm) with CH_2CH_2N (2.7 – 2.9 ppm).

3.3.2 Size and Z-potential of PEGylated complexes

Size and zeta potential of PEG-PEIpDNA complexes formed in water at N/P ratio of 5 were investigated by Zetasizer Nano-ZS. Results of DLS measurements indicate that PEGylated complexes were 133 ± 20 nm in size with a net charge of 27 ± 7 mV (Figure 2). The polydispersity index (PDI) was approximately 0.1, thus indicating narrow size distribution, high uniformity in particle size distribution and overall general homogeneity of the sample. The size and surface charge of the complexes are both important parameters for their interaction and entry into cells [19, 20]. Adding PEG molecules on PEI/DNA complexes led a decrease of size and a change in shape of the adsorbed polyplexes which affect their transfection capability [12].

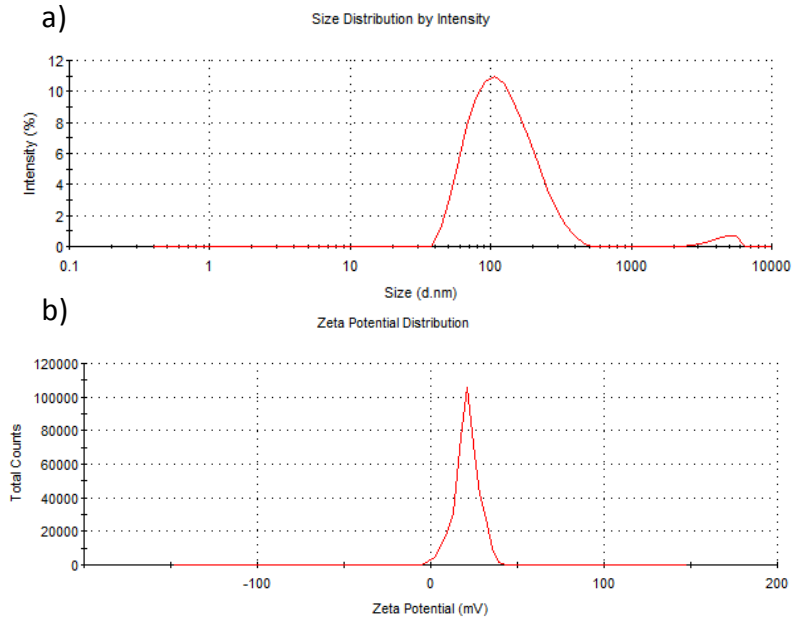

Figure 2 Representative dynamic light scattering (DLS) spectra. a) Hydrodinamic size distribution b) zeta-potential of PEG-PEI-DNA complexes at N/P ratio of 5 measured in double distilled water.

3.3.3 Characterization of complexes modified substrates

Morphology and distribution of PEG/PEIpDNA complexes adsorbed at glass substrates were assessed by atomic force and electron microscopy (AFM - SEM). SEM analysis of substrate surface have shown the circular morphology of the immobilized complexes and their surface distribution on glass substrates. In particular the figure 3, show an high density of complexes on substrate but indicate also a likely complexes aggregation, also as shown by the dimensions of fluorescent spots present on substrates in the cofocal images (Figure 4)

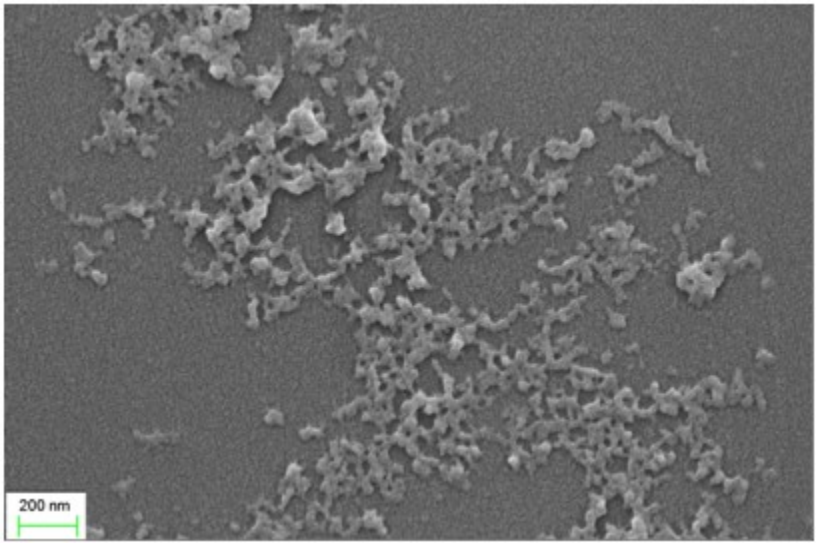

Figure 3 SEM images of PEGylated complexes adsorbed to a glass substrate.

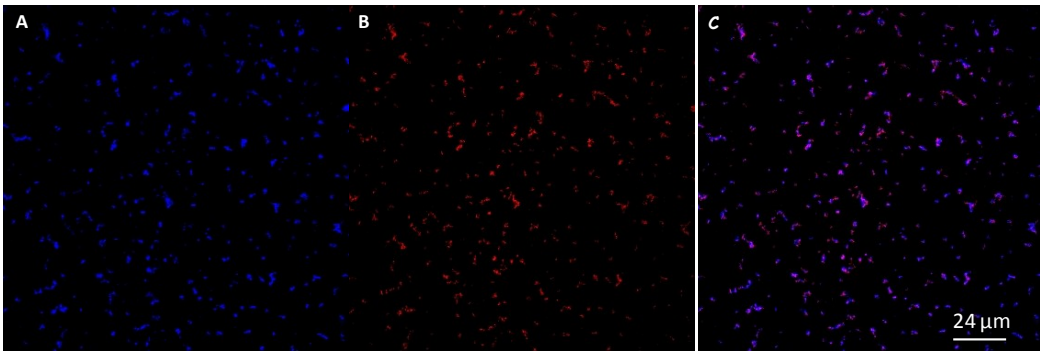

Figure 4 CLSM images of PEGylated complexes adsorbed to a glass substrate. (A) DNA-Cy5, (B) PEI-Rhod, (C) merge of A and B images.

Scanning of the substrates with different amounts of adsorbed complexes by atomic force microscopy (AFM), has displayed the different distribution of adsorbed complexes on the two kind of samples (1 – 2 µg DNA), but also the presence of larger aggregates on substrates with greater amount of immobilized complexes (Fig. 5). The 3D projections of the AFM images highlight the feature heights of the complexes adsorbed on substrates, in particular, the adsorption of 1 µg or 2 µg DNA complexes produce surface protrusions with average heights of 110 nm and 240 nm, respectively. The latter height values of adsorbed complexes are bigger than the characteristic diameter of PEGylated complexes (ca. 100-150 nm) [21, 22], the differences are most likely due to the formation of aggregates caused by the method of DNA complexes immobilization [23, 24].

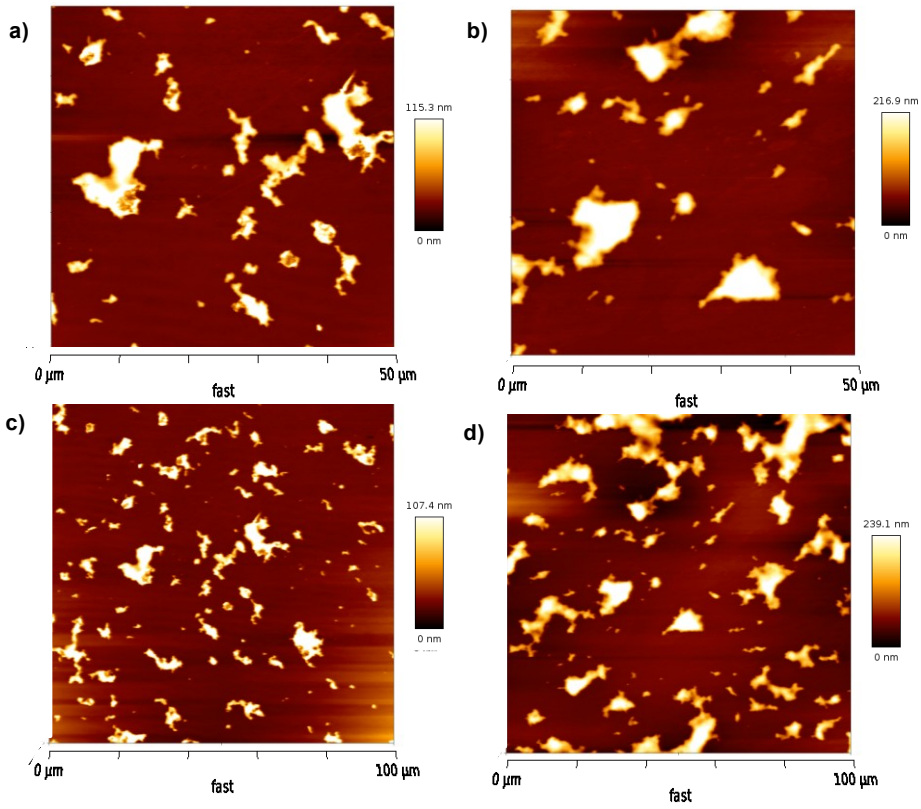

Figure 5 AFM images of complexes modified substrates. a) and c) 1 µg DNA complexes immobilized to glass substrate images at 50 µm and 100 µm magnification, respectively. b) and d) 2 µg DNA complexes adsorbed to substrate images at 50 and 100 µm of magnification, respectively

3.3.4 Complexes adsorption efficiency

Complexes adsorption efficiency was calculated monitoring DNA complexes concentration, before and after immobilization process, by fluorescence measures of the DNA-Cy5 complexes present in solution. Results in table 1 indicate that varying the experimental DNA concentrations, the percentage of the PEGylated complexes immobilized at the surface of the glass substrates is on average 67 ± 3 % concerning the amount of DNA complexes initially measured and incubated on substrates. Therefore, the surface density that complexes can cover changes with the DNA concentration at which the complexes are formed. Probably, high

concentrations of complexes in solution involve their aggregation that prevents the interaction with substrate, resulting in lower adsorption efficiency.

C_i (ng/uL)	μg_i DNA	C_f (ng/uL)	% Adsorption	Surface Density ($\mu g/cm^2$)
6	0.5	0.75	87	0.43
12	1	3	70	0.7
19	1.5	6	68	1.02
24	2	8.5	65	1.22

Table 1 Adsorption efficiency of PEGylated complexes to glass substrates. C_i initial concentration of complexes before adsorption process, μg_i DNA quantities applied to the substrates before immobilization, C_f concentration of unbound complexes solution, % adsorption calculating as different percentage between the two concentration values

3.3.5 Transfection efficiency

Substrate-mediated transfection by PEGylated complexes adsorbed at glass substrates is influenced by DNA density immobilized on substrate. The percentage of transfected NIH3T3 cells by surface-adsorbed complexes increased with the amount of immobilized DNA-complexes (1 – 2 μg DNA) [Fig. 6 a]. Transfection efficiency was depends upon an appropriate balance between the time of exposure of the cells to complexes modified substrates and the amount of immobilized DNA. At 24 h transfection not occur for the samples with lower amount of DNA complexes adsorbed (1ug). Maximal number of transfected cells (26%) were observed with the highest quantity of surface-bound complexes (2 μg) in 48 h. For bolus delivery (Fig.6 b), addition of 0.7 μg of DNA complexes, which correspond to the effective amount of complexes adsorbed on substrate with lower DNA concentration, assure a transfection of 20% of the cell population in 48 h. This

value of transfection efficiency is reached in 24 h with 1.4 µg of DNA complexes, which correspond to higher complexes functionalization of the substrate, added free in the control samples.

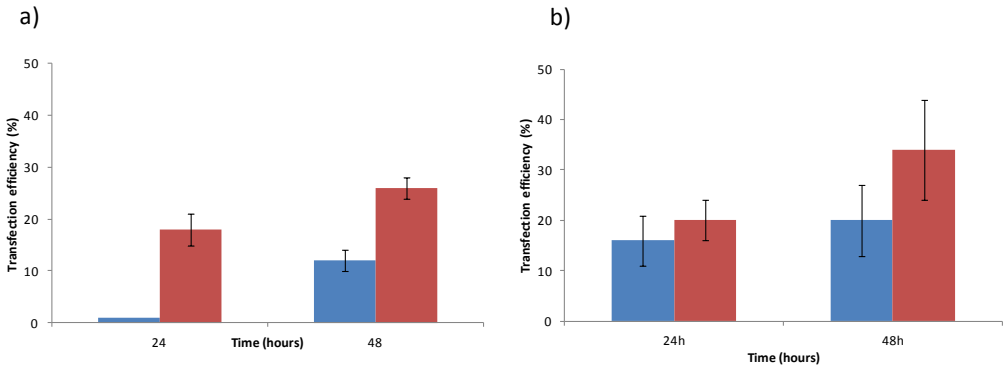

Figure 6 Comparison of transfection efficiency by a) bolus and b) substrate-mediated delivery. blue bar for lower amount of complexes immobilized (1µg) or added free (0.7µg) in solution. red bar for higher amount of complexes immobilized (2µg) or free (1.4 µg) added free in solution

3.3.6 Quantification and localization of internalized complexes

To estimate the fraction of DNA complexes internalized by cells plated on modified substrates, NIH3T3 cells was detached from substrates at different time points, reseeded on inert dishes and fixed after 24 h. Fluorescence of intracellular complexes was monitored in time by CLSM analysis, and the amount of the DNA-Cy5 complexes internalized, calculated by images elaboration, was expressed as the percentage area of the cells occupied by internalized complexes. Nearly all cells on surfaces with immobilized complexes had internalized DNA, at the same time, for substrate-mediated delivery, the majority of DNA complexes remained immobilized to the surface. Moreover, intracellular fluorescence of the internalized complexes was monitored at different time points (figure 7) . Results indicate that intracellular fluorescence increase until 48 h culture on complexes modified

substrates, no statistical variations were detect after this time point. This observation suggest a possible substrate release of complexes before cellular uptake.

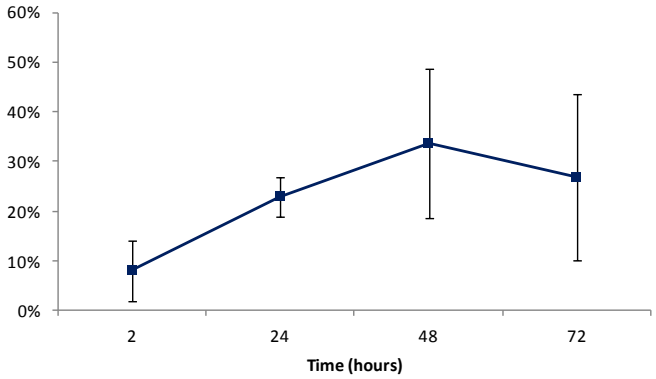

Figure 7 Quantification of internalized complexes by the cells seeded on modified substrates. Percentage cellular area occupied by internalized complexes during time

We subsequently characterized the quantity of intracellular complexes co-localized with lysosomes. DNA complexes and lysosomes were imaged by confocal microscopy. The co-localization of DNA into lysosomal compartments was estimated by Pearson's coefficient which describe how well are the DNA-Cy5 and lysosome-Rhod relate by a linear equation, if it will be equal to 1 all Cy5 voxels are exactly double in intensity than the Rhod ones. Taking in account this definition, we can conclude that for both samples and controls Pearson's coefficient values indicate a lower percentage of internalized complexes co-localized with lysosomes (table 2)

	Pearson's coefficient
Sample_adsorbed complexes	0,47 ± 0,13
Ctrl_free complexes	0,37 ± 0,1

Table 2 Pearson's coefficient values

3.4 References

1. Niidome, T. and L. Huang, *Gene therapy progress and prospects: nonviral vectors.* Gene Ther, 2002. **9**(24): p. 1647-52.
2. Varga, C.M., K. Hong, and D.A. Lauffenburger, *Quantitative analysis of synthetic gene delivery vector design properties.* Mol Ther, 2001. **4**(5): p. 438-46.
3. Pannier, A.K., B.C. Anderson, and L.D. Shea, *Substrate-mediated delivery from self-assembled monolayers: effect of surface ionization, hydrophilicity, and patterning.* Acta Biomater, 2005. **1**(5): p. 511-22.

4. Pannier, A.K. and L.D. Shea, *Controlled release systems for DNA delivery.* Mol Ther, 2004. **10**(1): p. 19-26.
5. Luo, D. and W.M. Saltzman, *Enhancement of transfection by physical concentration of DNA at the cell surface.* Nat Biotechnol, 2000. **18**(8): p. 893-5.
6. Levy, R.J., et al., *Localized adenovirus gene delivery using antiviral IgG complexation.* Gene Ther, 2001. **8**(9): p. 659-67.
7. Segura, T. and L.D. Shea, *Surface-tethered DNA complexes for enhanced gene delivery.* Bioconjug Chem, 2002. **13**(3): p. 621-9.
8. Fishbein, I., et al., *Site specific gene delivery in the cardiovascular system.* J Control Release, 2005. **109**(1-3): p. 37-48.
9. Segura, T., M.J. Volk, and L.D. Shea, *Substrate-mediated DNA delivery: role of the cationic polymer structure and extent of modification.* J Control Release, 2003. **93**(1): p. 69-84.
10. Adler, A.F. and K.W. Leong, *Emerging links between surface nanotechnology and endocytosis: impact on nonviral gene delivery.* Nano Today, 2010. **5**(6): p. 553-569.
11. Delehanty, J.B., K.M. Shaffer, and B. Lin, *A comparison of microscope slide substrates for use in transfected cell microarrays.* Biosens Bioelectron, 2004. **20**(4): p. 773-9.
12. Pannier, A.K., J.A. Wieland, and L.D. Shea, *Surface polyethylene glycol enhances substrate-mediated gene delivery by nonspecifically immobilized complexes.* Acta Biomater, 2008. **4**(1): p. 26-39.
13. Ludtke, J.J., M.G. Sebestyen, and J.A. Wolff, *The effect of cell division on the cellular dynamics of microinjected DNA and dextran.* Mol Ther, 2002. **5**(5 Pt 1): p. 579-88.
14. Kursa, M., et al., *Novel shielded transferrin-polyethylene glycol-polyethylenimine/DNA complexes for systemic tumor-targeted gene transfer.* Bioconjug Chem, 2003. **14**(1): p. 222-31.

15. Nguyen, H.K., et al., *Evaluation of polyether-polyethyleneimine graft copolymers as gene transfer agents.* Gene Ther, 2000. **7**(2): p. 126-38.
16. Boussif, O., et al., *A versatile vector for gene and oligonucleotide transfer into cells in culture and in vivo: polyethylenimine.* Proc Natl Acad Sci U S A, 1995. **92**(16): p. 7297-301.
17. Costes, S.V., et al., *Automatic and quantitative measurement of protein-protein colocalization in live cells.* Biophysical journal, 2004. **86**(6): p. 3993-4003.
18. Tang, G.P., et al., *Polyethylene glycol modified polyethylenimine for improved CNS gene transfer: effects of PEGylation extent.* Biomaterials, 2003. **24**(13): p. 2351-62.
19. Bettinger, T., J.S. Remy, and P. Erbacher, *Size reduction of galactosylated PEI/DNA complexes improves lectin-mediated gene transfer into hepatocytes.* Bioconjug Chem, 1999. **10**(4): p. 558-61.
20. Oku, N., et al., *The fusogenic effect of synthetic polycations on negatively charged lipid bilayers.* J Biochem, 1986. **100**(4): p. 935-44.
21. Tseng, S.J., C.J. Chuang, and S.C. Tang, *Electrostatic immobilization of DNA polyplexes on small intestinal submucosa for tissue substrate-mediated transfection.* Acta Biomater, 2008. **4**(4): p. 799-807.
22. Bengali, Z., et al., *Gene delivery through cell culture substrate adsorbed DNA complexes.* Biotechnol Bioeng, 2005. **90**(3): p. 290-302.
23. Petersen, H., et al., *Polyethylenimine-graft-poly(ethylene glycol) copolymers: influence of copolymer block structure on DNA complexation and biological activities as gene delivery system.* Bioconjug Chem, 2002. **13**(4): p. 845-54.
24. Merdan, T., et al., *PEGylation of poly(ethylene imine) affects stability of complexes with plasmid DNA under in vivo conditions in a dose-dependent manner after intravenous injection into mice.* Bioconjug Chem, 2005. **16**(4): p. 785-92.

Chapter 4

Specific adsorption of PEI/DNA complexes to fibronectin coated substrate through a peptide linker.

4.1 Introduction

The opportunity to enhance gene transfer, characteristic of controlled delivery systems, is due to retention of elevated DNA concentration within the cellular microenvironment. The continued presence of the exogenous DNA during cell division, indeed, may also facilitate entry into the nucleus, during which the nuclear membrane is compromised [1]. Substrate-mediated delivery, in particular, involve the immobilization of gene vectors to a substrate that support cell adhesion, allowing for cellular internalization and reducing aggregation and mass transport limits [2]. Several strategies have been employed to associate DNA complexes with the substrate, including entrapment in gelatin followed by addition of the transfection reagent [3], poly-electrolyte layering of DNA [4], specific tethers through the biotin-avidin interaction [5-7] or non specific adsorption [8]. When delivered from a surface, the ability of nonviral particles to induce gene expression depends not only on their local concentration, but also on the tightness of their adsorption, on substrate surface chemistry, and on the presence of extracellular matrix (ECM) proteins [9]. DNA complexes can be adsorbed on uncoated substrate [10-14] or substrates coated with serum or extracellular matrix proteins to mediate cell adhesion and complex immobilization [15]. Gene transfer using collagen, for instance, is hypothesized to function by maintaining the DNA in situ, possibly due to limited transport through the collagen, until internalization by cells present locally [16, 17]. A similar strategy has been used by some viruses, which associate with extracellular matrix molecules (e.g., fibronectin) for enhanced uptake [18, 19]. More recently, synthetic systems that specifically bind viruses [20, 21] or nonviral DNA complexes [5] to a polymeric substrate are being developed. Manipulating the surface properties of a material through the adsorption of proteins, such as serum, mediates both DNA complex binding and cellular adhesion. Serum exposure on tissue-culture polystyrene substrates (TCPS) results in adsorption of fibronectin that supports cell adhesion [22], and immobilization of non-viral

vectors to the adsorbed proteins enhances gene transfer from the surface relative to no coating substrate [15]. Individual proteins or protein mixtures, such as serum, fibronectin, collagen, or laminin, are routinely deposited onto biomaterials to support cell adhesion [23-26]. In addition to mediating cell attachment and the immobilization of vectors, protein pre-adsorbed to surfaces, also used in reverse transfection, can improve transgene expression. The protein coating can potentially interface with cellular processes to direct internalization and intracellular trafficking [27-29]. Complexes delivered with protein may maintain conformations favorable for cellular uptake, or may be differentially trafficked. Several studies demonstrate that fibronectin deposited onto solid support dramatically increase the reverse transfection efficiency of polyplexes [8] and mediate the greatest levels of transgene expression compared to other extracellular matrix (ECM) proteins [15], which suggests an active role of fibronectin in the internalization and intracellular trafficking of gene complexes. Fibronectin is internalized by a caveolin-dependent pathway [29], and thus vectors associated with fibronectin may similarly be internalized via caveolae-mediated endocytosis [30]. Thus, the ECM protein targets the vector toward a specific internalization pathway that can influence the ultimate fate of the vector, as internalization via caveolae-mediated endocytosis may avoid the lysosome and subsequent degradation relative to internalization via clathrin mediated endocytosis [27, 28].

Taking advantage of the adhesive properties and increased transfection efficiency induced by fibronectin coating, in this preliminary study we have specifically adsorbed DNA complexes to a solid substrate. In order to obtain a specific interaction between DNA complexes and fibronectin coated substrates, we have used a peptide linker with specific affinity for this protein. Several studies have shown fibronectin binding activity of synthetic peptides containing motifs, sites or some amino acids with particular affinity for a specific domain of the adhesion protein [31]. In particular, human plasma fibronectin was found to bind unexpectedly avidly to a 17 amino acid peptide (KRFKQDGGWSHWSPWSS)

from the second type I repeat of thrombospondin, an extracellular matrix glycoprotein. Roberts et al. have identified a hexapeptide (GGWSHW) within this sequence that accounts for this interaction. Furthermore, the peptide is a potent inhibitor of fibronectin binding to gelatin and of fibronectin-mediated cell adhesion to a gelatin or collagen matrix [31], which suggest the primarily interaction with the gelatin-binding domain of fibronectin. In this work, we have specifically immobilize PEI/DNA complexes to fibronectin coated substrates through the hexapetide GGWSHW, evaluating the effective affinity to fibronectin compared to a control peptide. Moreover, peptide has been conjugated with polyethylenimine (PEI), the product of this conjugation was adsorbed to fibronectin layer to allow the specific adsorption of PEI/DNA complexes. Finally, we have proposed a simple way to pattern the surface with fibronectin spots to create adhesive/transfective islands on solid substrate.

4.2 Materials and Methods

4.2.1 Materials

Linear Polyethylenimine (L-PEI) with an average molecular weight of 25 kDa was purchased from Polysciences (Warrington, PA). Tetramethylrhodamine-conjugated linear PEI (JetPEI-fluoR) were purchased from Polyplus-transfection SA (7mM ammine content, Illkirch, France). The reporter plasmid encoding for enhanced green fluorescent protein (EGFP) driven by a cytomegalovirus (CMV) promoter was amplified in *E. coli*, extracted and purified from bacteria culture using Qiagen plasmid kit (Santa Clara, CA). Preliminary cellular adhesion studies were

performed with mouse embryo fibroblasts (NIH3T3), cultured at 37 °C and 5% CO_2 in Dulbecco's modified Eagle medium with 4,5 g L^{-1} glucose (DMEM, Gibco) supplemented with 10% Bovine Calf Serum (BCS, Gibco), 4 mM glutamine, 100 U mL^{-1} penicillin and 0.1 mg mL^{-1} streptomycin. For imaging, plasmid DNA (p^{CMV}EGFP) was labeled with the cyanine dye Cy5 using Label IT® Tracker™ Intracellular Nucleic Acid Localization Kit purchased from Mirus Bio (Madison, WI, USA). Fibronectin from bovine plasma was purchased from Sigma Aldrich (St. Louis, MO, USA). Reagents for peptides synthesis (Fmoc-protected amino acids, resins, activation, and deprotection reagents) were obtained from Iris Biotech GmbH (Waldershofer Str. 49-51 95615 Marktredwitz, Deutschland) and InBios (Naples, Italy). Solvents for peptides synthesis and HPLC analyses were purchased from Sigma-Aldrich; reversed phase columns for peptide analysis and the LC–MS system were supplied respectively from Agilent Technologies and Waters (Milan, Italy). All chemicals were used as received.

4.2.2 Peptides synthesis

Solid phase peptide synthesis of fibronectin-adhesive peptide (6 aa) and control peptide (13 aa) was performed on a fully automated multichannel peptide synthesizer Biotage® Syro Wave™. The 6-mer and 13-mer peptides were synthesized in the amidate version, employing the solid phase method on a 50 μmol scale following standard Fmoc strategies. Rink-amide resin (substitution 0.45 mmol/g) was used as solid support. Activation of amino acids was achieved using HBTU/HOBt/DIPEA (1:1:2). All couplings and deprotections were performed for 15 and 10 min, respectivetly. Peptides were then removed from the resin, by treatment with a TFA/TIS/H_2O (95:2.5:2.5, v/v/v) mixture for 90 min at room temperature; then, crude peptides were precipitated in cold ether, dissolved in a water/acetonitrile (1:1, v/v) mixture, and lyophilized. Product were purified by

preparative RP-HPLC on a Waters 2535 Quaternary Gradient Module, equipped with a 2489 UV/Visible detector and with an X-Bridge^{TM} BEH300 preparative 10 × 100 mm C8, 5μm column, applying a linear gradient of 0.1% TFA CH_3CN in 0.1% TFA water from 5% to 70% over 30 min at a flow rate of 5 mL/min. Peptides purity (97%) and identity was confirmed by LC–MS analyses carried out on an Agilent 6530 Accurate-Mass Q-TOF LC/MS spectrometer with Zorbax RRHD Eclipse Plus C18 2.1 x 50 mm, 1.8 μm columns. Purified peptide were lyophilized and stored at −20 °C until use.

4.2.3 Surface Plasmon Resonance

The interactions between fibronectin with 6-mer peptide and 13-mer peptide were measured using the SPR technique with SensiQ Pioneer from AlfaTest (Rome, Italy). In order to measure the affinity of the peptides (analyte) with the protein (ligand), fibronectin was immobilized at a concentration of 10 μg/mL in a 10 mM acetate buffer pH 4.5 (flow 10 μL/min, injection time 20 min) on a COOH1 SensiQ sensor chip, using EDC/NHS chemistry (0.4 M EDC - 0.1 M NHS, flow 25μl/min, injection time 4 min), achieving a 1900 RU signal. Groups reactive residues were deactivated by treatment with ethanolamine hydrochloride 1 M, pH 8.5. The reference channel was prepared by activation with EDC/NHS and deactivation with ethanolamine. The binding assays were performed at 25 μL/min, with a contact time of 4 min, the 6-mer and 13-mer peptides were diluted in the buffer stroke, HBS (10 mM Hepes, 150 mM NaCl, 3 mM EDTA, pH 7.4).The injection of analytes (100 μL) was performed at the indicated concentrations. The association phase (k_{on}) was followed for 180 s, whereas the dissociation phase (k_{off}) was followed for 300 s. The complete dissociation of formed active complex was achieved by addition of 10 mM NaOH, for 60 s before each new cycle start. To

subtract the signal of the reference channel and evaluate the kinetic and thermodynamic parameters of the complex, the software QDAT analysis package (SensiQ Pioneer, AlfaTest) was used. For 6-mer peptide same experiment was conducted by One step injection as well. In this case an analyte concentration of 826 μM was used with a flow rate of 25 μL min^{-1} and a 600 sec of dissociation time. In this experiment the volume of sample was configured as a percentage of the dispersion loop volume, so in order to have a longer plateau at full concentration the largest percentage (100%) was used. As to bulk standard cycles, a 3% of sucrose was used. For all experiments, kinetic parameters for both peptides (hexa- and control peptide) were estimated assuming a 1:1 binding model and using QDAT software (SensiQ Technologies).

4.2.4 Specific adsorption of hexapeptide to fibronectin

In order to demonstrate the specific adsorption of 6-mer peptide to a fibronectin layer, a fixed peptide concentration solution (70 μM) was analyzed before and after adsorption process by RP-HPLC, following tryptophan signal at 280nm. The indicated amounts of protein were diluted in phosphate buffered saline (PBS), added to glass slides of 12 mm diameter (Knittel glass, Germany) and incubated for 2 hours. In particular, the adsorption of the same concentration of the 6-mer peptide (70 μM) was tested on three different fibronectin coating concentrations (10 – 30 – 50 μg mL^{-1}) and on uncoated glass substrate, as control.

4.2.5 PEI-peptide conjugation

In order to synthesize a peptide–polymer hybrid a solid phase chemical synthesis method was used. Immediately after peptide synthesis, the amine group of the last

glycine residue of the hexapeptide (GGWSHW) was activated for 1 h by disuccimidyl carbonate (DSC, Sigma Aldrich) on the resin support in a synthesis column, while the side chains of other peptide residues were still protected. After washing the column to remove excess DSC, the activated peptide was mixed with a small excess of PEI 25 kDa (Polyscience, SA) and the two compounds were allowed to react for overnight. The column was washed again to remove free PEI. The peptides were then deprotected, cleaved from the resin, and precipitated with ether. The crude complex was purified by RP-HPLC as previously described for peptide purification. Since PEI is not detected by ESI-QTOF, HPLC most relevant peaks were tested by proton nuclear magnetic resonance spectrometry (^{1}H-NMR). HPLC fractions were lyophilized and resuspended in H_2O/D_2O mixture for NMR analysis. ^{1}H-NMR spectra were recorded on an Agilent 600 MHz spectrometer equipped with a DD2 console and a OneNMRprobe. The formed complex (Figure 1) was tested by RP-HPLC, monitoring peptide and PEI UV signal, using a linear gradient as previously described. The same procedures were performed for the conjugation of PEI to peptide control.

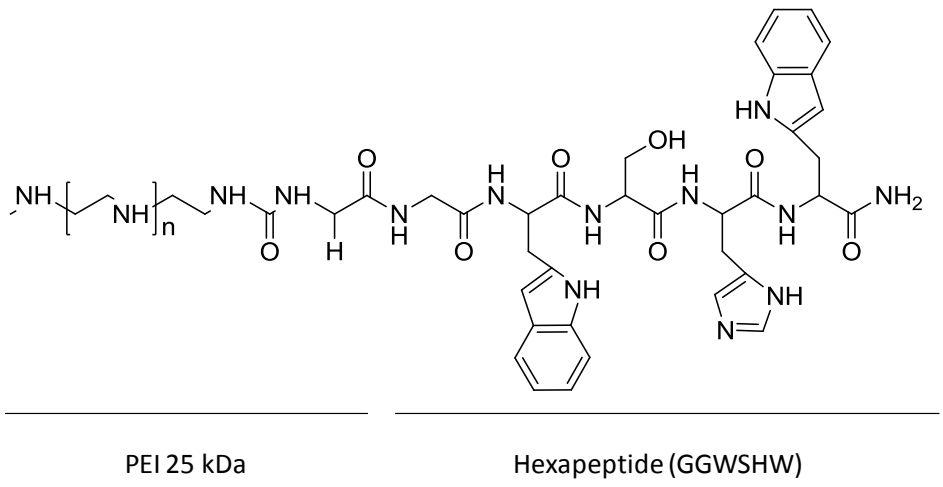

Figure 1 Chemical structure of PEI 25 kDa conjugated to 6-mer peptide through the formation of an amide bond

4.2.6 Substrate coating, PEI/DNA complexes formation and immobilization

To preliminary test the co-immobilization of PEI-peptide and PEI/DNA complexes, a fibronectin layer was immobilized to glass coverslips (Φ 12 mm) by 2 h incubation. After protein adsorption, substrates were washed with 1 X PBS and further incubated for 2 h with PEI-peptide conjugate dissolved in water at final concentration of 16 μM. PEI/DNA complexes were formed in 150 mM NaCl at an N/P ratio of 5, adding PEI solution dropwise to a solution containing DNA, vortexed for 10 s and incubated for 15 min at room temperature [32]. Complexes, 1 μg DNA for substrate, were immobilized by incubation on fibronectin coated glass slides modified with PEI-hexapeptide for 2 h and were then washed twice with 1 X PBS. In order to imaged cell on this substrates, 5000 cells were seeded on specifically adsorbed complexes to fibronectin coated glass substrates. After 24 h, samples were fixed with 4 % paraformaldehyde (Sigma Aldrich), and actin staining was performed by incubating samples with TRITC-phalloidin (Sigma) in PBS for 30 min at room temperature.

4.2.7 Indirect immunofluorescence

Indirect immunofluorescence was performed on samples after cells plated on PEI/DNA complexes adsorbed specifically to through linker hexapeptide to detect fibronectin coat. The samples, prepared as described above, were incubated with 0.5 % (w/v) bovine serum albumin (BSA, Sigma Aldrich) dissolved in phosphate buffer saline solution (PBS) for 30 min at RT to prevent non specific staining.

Then, they were stained by incubation for 1 h at RT with a specific mouse monoclonal antibody (Sigma Aldrich) with affinity for the fibronectin cell binding domain diluted at 1:200 in PBS 0.5 % BSA. Bound antibodies were revealed by incubation for 1 h with 1:500 Alexa-fluor 488 anti-mouse secondary antibodies (Invitrogen, Life Technologies) diluted in PBS 0.5 % BSA. After rinsing in 1 X PBS, the samples were investigated with a Leica TCS SP5 II confocal laser microscope, equipped with an argon laser, at a wavelength of 488 nm, and a HeNe laser, at a wavelength of 543 nm and 633 nm. Images were acquired with 25x objective at resolution of 1024 x 1024 pixel.

4.2.8 Generation of adhesive/transfective islands

In order to built adhesive/transfective islands, 500 μm diameter spots of protein was obtained through the stamp of fibronectin on glass slides. For the stamp fabrication, the negative of micropillars array (stamp) was tooled from a PMMA substrate by using the micro-milling technique (Mini-Mill/GX, Minitech Machinery Corporation), to form a cylindrical cavity with a diameter of 500 μm and a depth of 200 μm. Then, a flexible layer with micropillars was obtained by pouring poly(dimethylsiloxane) (PDMS, Dow Corning 184 Sylgard), mixed in ratio 10:1 with curing agent on the above described master and under vacuum until complete disappearance of the air bubbles. Finally, PDMS was cured at 80 °C for 30 min and peeled off from PMMA master. The quality of the stamps obtained was investigated under a microscope. The desired stamps were then placed in an ultrasonic bath containing 70% ethanol for 5 min for sterilization and then dried under a flow of nitrogen gas [33]. After drying, a plasma cleaner (Femto, Diener, Böblingen, Germany) was used to remove the surface layer of organic compounds and oxidize the surface of PDMS stamps. To print of the protein of glass surface, stamps were inked with 20 μl of fibronectin 50 μg ml^{-1}, the solution was left at

room temperature for 10 min in order to bind protein to the surface of the stamp. Once the incubation was complete, the stamps were then immediately placed into contact with a glass coverslips for 10 s, then peeled off and the printed coverslip was dried for 2 h [34].

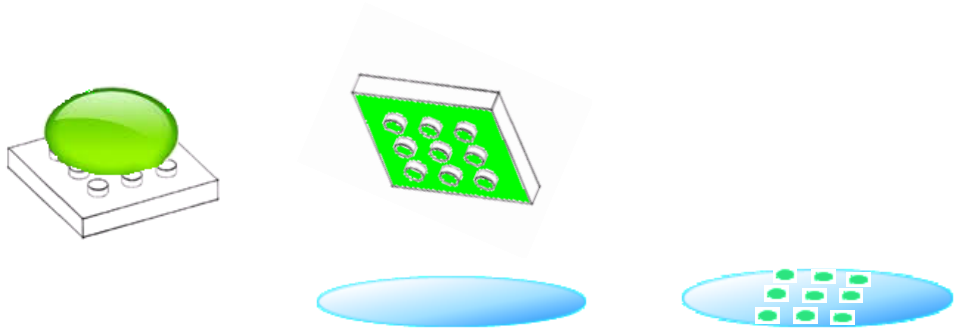

Figure 2 Scheme of protein patterning strategy use to generate adhesion island cultures. The stamp was inked with fibronectin solution, before printing the protein onto a glass slide.

4.3 Results and Discussions

4.3.1 Peptide synthesis

6-mer and 13-mer peptides used to test fibronectin affinity were chemically synthesized with good yields by SPPS, using Fmoc methodologies as C-terminal amidated derivatives and purified by RP-HPLC. Their identity and purity (averaged purity > 97%) were assessed by LC–MS. The table 1 show the amino acid sequences of two peptides, with expected and experimental molecular weight. The figures 3a and 3b display the LC–MS spectra of crude and pure hexapeptide,

respectively. Whereas, figures 4a and 4b show LC–MS spectra of crude and pure control peptide, respectively.

	Amino Acid Sequence	Theoretical MW (g mol^{-1})	Experimental MW (g mol^{-1})
6-mer peptide	GGWSHW	727.78	728.32
13-mer peptide	WKVDFEEDTLPKD	1620.78	1621.79

Table 1 Amino acid composition of fibronectin binding peptides with theoretical (th) and experimental (exp) molecular weights (MW)

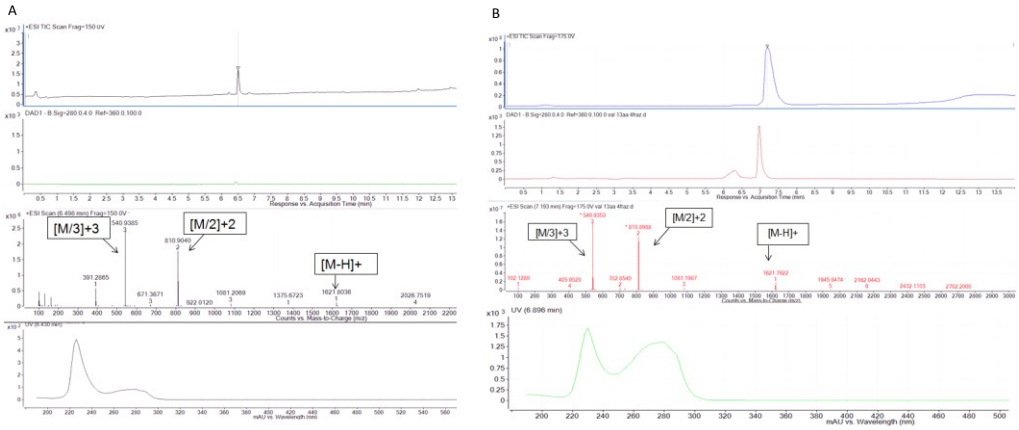

Figure 3 LC-MS analysis of 6-mer peptide. (A) LC-MS spectrum of crude peptide, (B) LC-MS spectrum of pure peptide

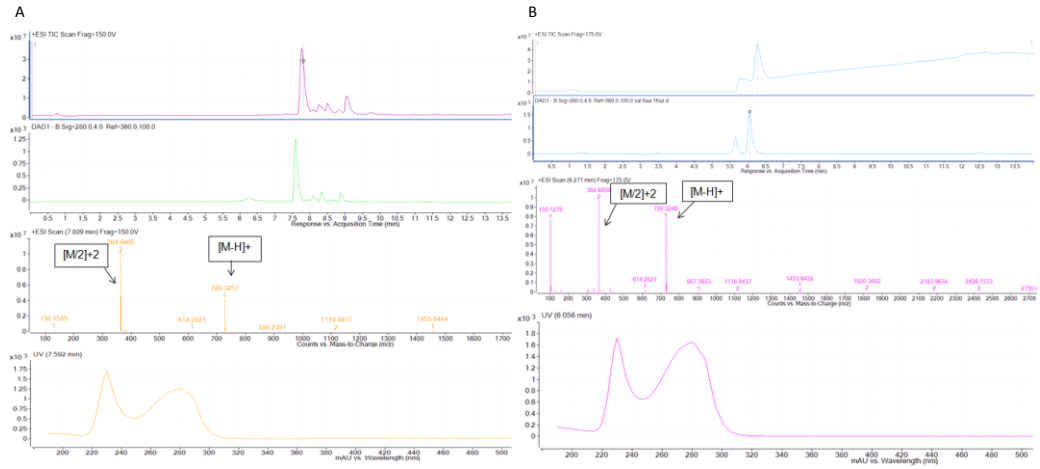

Figure 4 LC-MS analysis of 13-mer peptide. (A) LC-MS spectrum of crude peptide and (B) LC-MS spectrum of pure peptide

4.3.2. Hexapeptide-fibronectin binding affinity_SPR

Several synthetic peptides from fibronectin have been shown to inhibit interactions of fibronectin with cell surface integrin receptors [35] Previous investigations have shown that both hexapeptide (GGWSHW) and 13-mer peptide binds specifically fibronectin, in particular, the latter is part of a 38 amino acid long motif contained into membrane receptors of *Staphylococcus aureus* [36]. 6-mer and 13-mer peptide ability to bind fibronectin was evaluated by surface plasmon resonance (SPR) experiments. Fibronectin (ligand) was immobilized on COOH1 chip, achieving 1900 RU immobilization level, according to reported conditions (see Materials and Method section for details). Direct binding between fibronectin and 6-mer and 13-mer peptides were performed by injecting peptides solutions at increasing concentrations from 3µM to 826µM for shorter peptide and from 4.7 µM to 1.2 mM for the longer one. Only for 6-mer sequence a clear association to fibronectin

protein was shown by SPR technique as demonstrated by the dose-response overlay of sensorgrams reported in figure 5a.

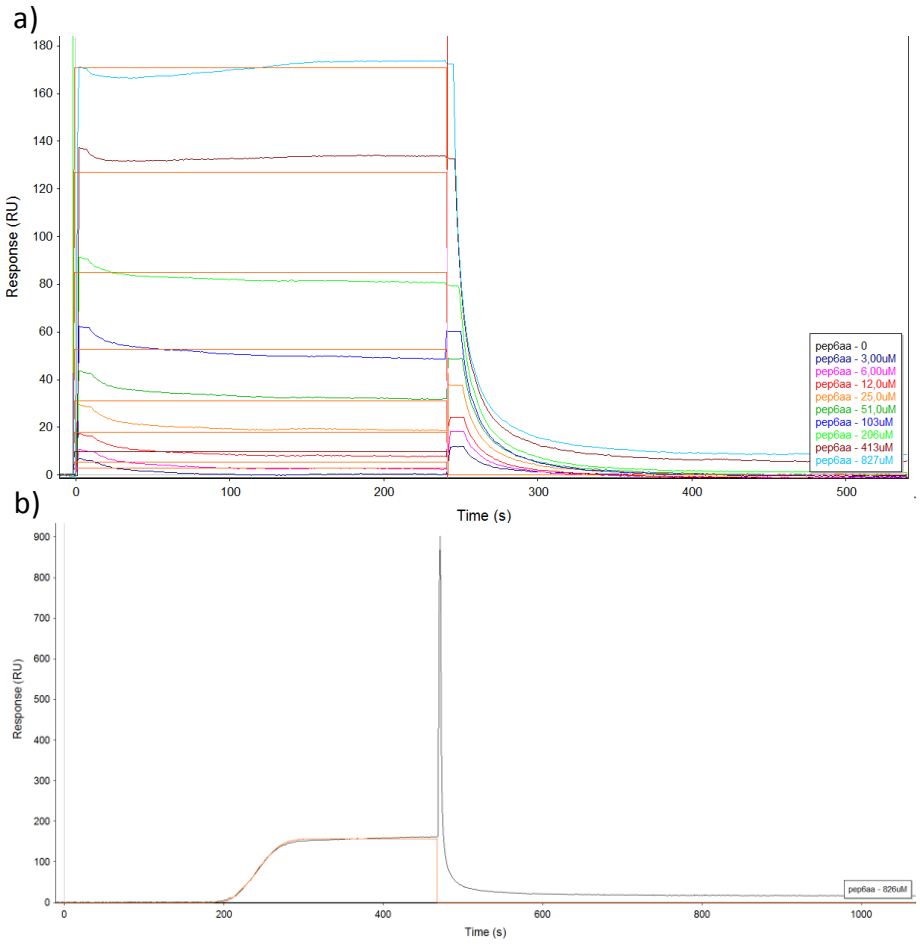

Figure 10 Binding of 6-mer peptide and fibronectin protein. a) Conventional SPR experiment, analyte concentration ranging from 3 µM to 826 µM. b) One Step injection, analyte concentration of 826 µM.

Employing a 1:1 interaction model, a low micromolar dissociation value for 6-mer peptide/fibronectin complex was shown. A good fitting was obtained using a 1:2 interaction model, suggesting the presence on fibronectin sequence of two different

binding sites for 6-mer peptides. First site shows a higher and more specific affinity than the second one. (Table 2).

6-mer peptide		
Conventional method		
	K_D	R_{max}
1 site	490 ± 0.1 µM	256 ± 1
2 site	20 ± 0.2 µM	10 ± 2
One step		
	K_D	R_{max}
1 site	3.96 ± 0.09 mM	700 ± 0.1
2 site	32.6 ± 0.05 µM	36.8 ± 0.3
13-mer peptide		
Conventional method		
	K_D	R_{max}
1 site	900 ± 0.2 mM	69.7 ± 0.9

Table 2 Kynetic parameters for both peptides (hexa- and control peptide) for Conventional and One Step experiments

Using the same condition a One Step experiment was conducted as well. This kind of experiment is based on Taylor dispersion theory [37], so a unique concentration of peptide (826µM) was dispersed into running buffer directly in the flow cell in order to have a final sigmoidal profile.(Figure 5b). Employing a 1:1 interaction model, a low micromolar dissociation value for 6-mer peptide/fibronectin complex was shown, that was in according to conventional SPR experiment. Even with One Step injection, the presence of two binding sites (the first one with a higher affinity and the second with a weak affinity) was confirmed. While for 13-mer peptide

there is no a clear association to the protein, the figure 6 shows a typical aspecific sensorgram with a low millimolar dissociation value. This result probably suggest the importance of whole sequence, 38-mer peptide, for fibronectin binding.

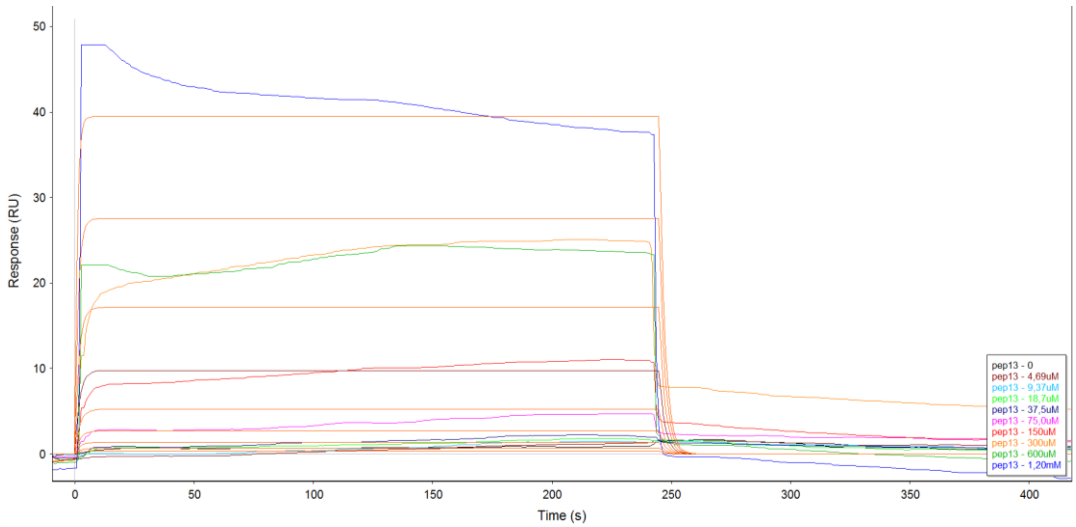

Figure 6 Binding of 13-mer peptide and fibronectin protein

4.3.3 Binding specificity

Adsorption specificity of peptide GGWSHW toward fibronectin was evaluated by RP-HPLC technique, measuring peptide concentration of unbound fraction after binding process. Three distintic layers of fibronectin at different concentrations (10 – 30 – 50 μg ml^{-1}) were used to test the specific adsorption of the 6-mer peptide at initial concentration of 70 μM. Figure 7 show three release profiles of the unbound peptide at different fibronectin layers. Higher peak reveal higher release from substrate with lower fibronectin concentration coat. While, lower peak show higher

adsorption to fibronectin coated substrate with higher concentration, therefore lower peptide concentration released.

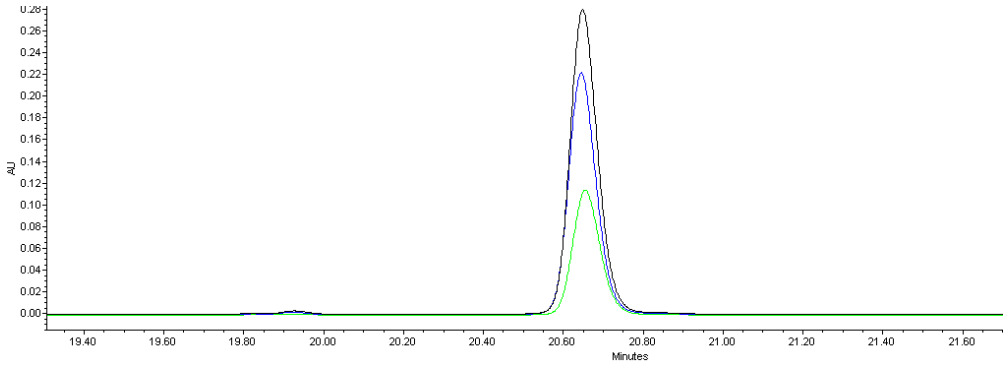

Figure 7 Reverse-phase-HPLC of 6-mer peptide specific binding on fibronectin coated glass. The chromatograms performed at 280 nm shows un bound peptide fractions at three different fibronectin layers. Black peak shows the 6-mer peptide release after incubation on 10 µg/mL fibronectin layer. unlike blue and green peaks show unbound peptide after binding with 30 and 50 µg/mL protein layers, respectively.

4.3.4 PEI-peptide conjugate characterization

The conjugation of the hexapeptide (GGWSHW) to linear PEI 25 kDa was confirmed by ^{1}H-NMR spectroscopy. Wang et al. reported that PEI metylen peak shifts from 2.5 to 3 ppm when it forms an amidic bond with the activated amino terminal group of the peptide. NMR spectrum of peptide-PEI is shown in fig. 8. A very intense peak is found at 3 ppm confirming the covalent binding of PEI to the peptide. Signals at around 10 ppm are typical of Trp indolic protons where signals in the region from 8 to6 ppm become to peptide backbond amide and side chains aromatic protons.

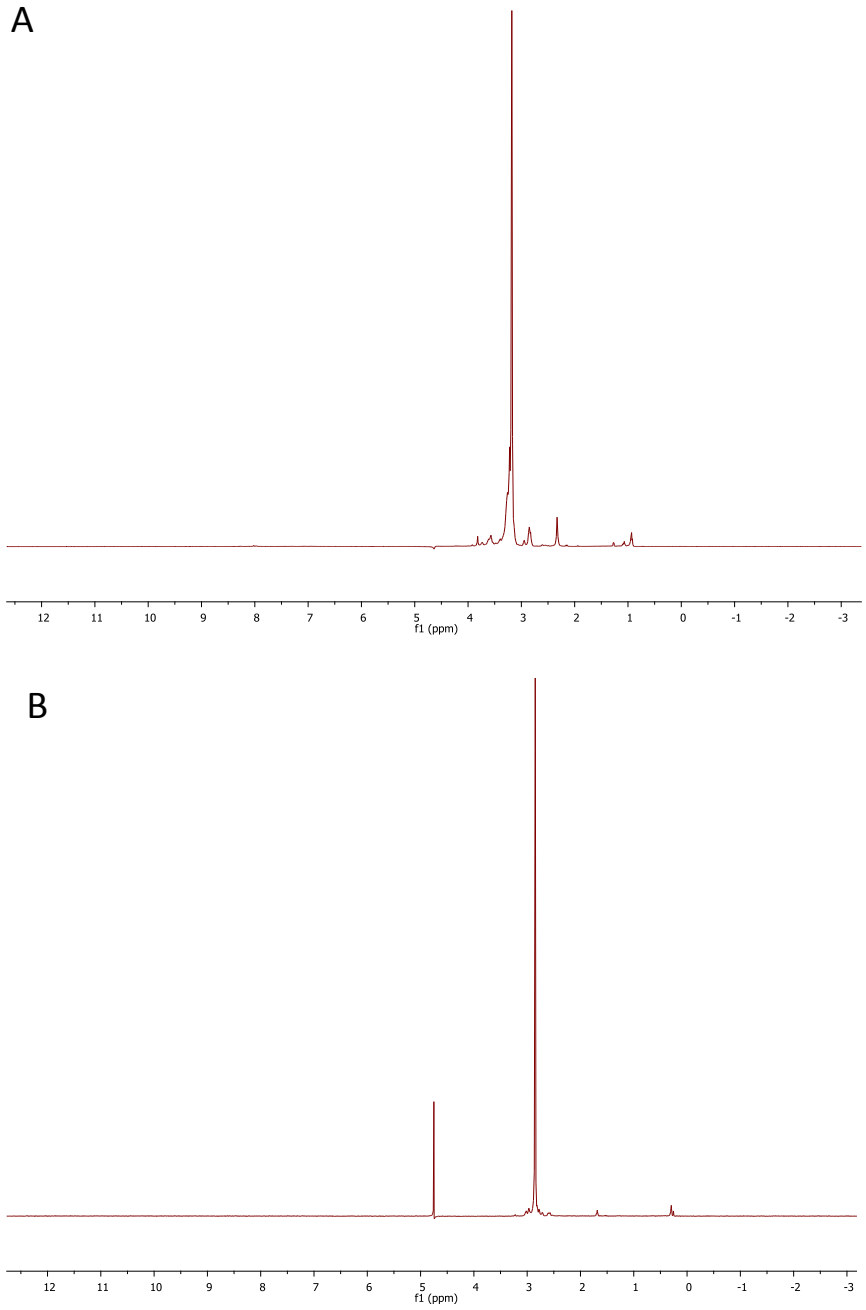

Figure 8 NMR spectra of PEI-6-mer and PEI-peptide complex. The shift of PEI peak (B) from 2.7 to 3.2 ppm confirms the correct covalent bond between peptides and polymer, the signals at 10 ppm and at 8-6 ppm typical of Trp residues and peptide backbone amide and side chains are visible in the spectrum (A).

The correct PEI-Peptide conjugation was confirmed by RP-HPLC, as well. In the figure 9 PEI-peptide crude complex chromatogram was reported. The presence of a non sharp peak at 230 nm that covers tryptophan peak at 280nm indicates the correct complex formation for both peptides.

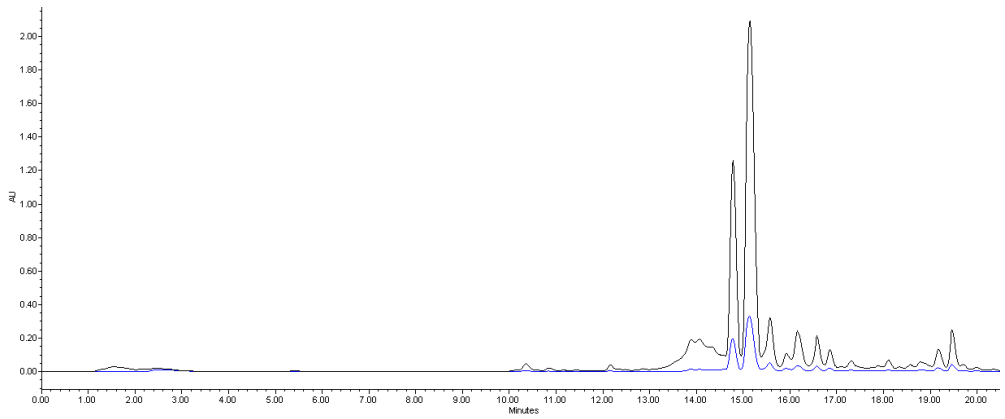

Figure 9 RP-HPLC analysis of PEI-peptide complex. a) 6-mer complex at 280 nm in blue and at 220 nm in black. The presence of a non sharpe peak at 220 nm confirms the correct formation of the complex that is not visible at 280 nm.

4.3.5 Imaging of PEI/DNA complexes specifically adsorbed to fibronectin coated substrates and adhesive/transfective islands

Results of immunofluorescence on samples with cells seeded on PEI/DNA complexes specifically adsorbed to fibronectin coated substrates and fibronectin stamps to glass slides such as adhesive islands were shown in the figure 10 and 11. Figures show blue spots of PEI/DNA complexes adsorbed to green layer/spots of fibronectin and cell seeded on this system with red cytoskeleton.

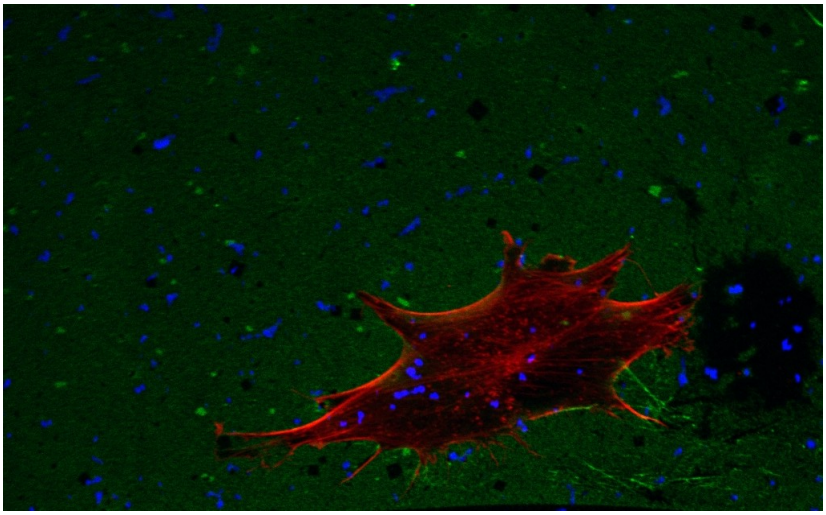

Figure 10 CLSM image of cell on complexes specifically adsorbed to fibronectin coated substrate through linker 6-mer peptide

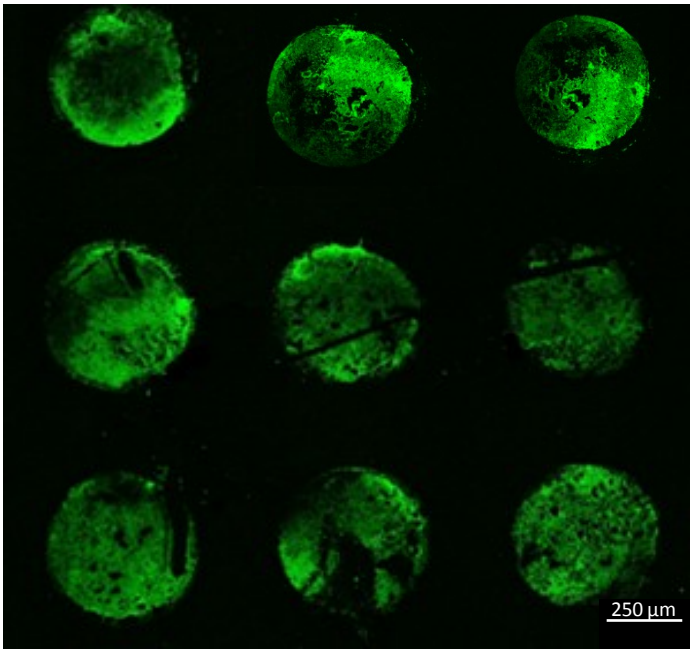

Figure 11 CLSM image of array of printed fibronectin spots. 3×3 array of 500 um diameter islands of fluorescently labeled IgG generated by contact printing

4.4 References

1. Tseng, W.C., F.R. Haselton, and T.D. Giorgio, *Mitosis enhances transgene expression of plasmid delivered by cationic liposomes.* Biochim Biophys Acta, 1999. **1445**(1): p. 53-64.
2. Bengali, Z., et al., *Efficacy of immobilized polyplexes and lipoplexes for substrate-mediated gene delivery.* Biotechnol Bioeng, 2009. **102**(6): p. 1679-91.
3. Ziauddin, J. and D.M. Sabatini, *Microarrays of cells expressing defined cDNAs.* Nature, 2001. **411**(6833): p. 107-10.
4. Jewell, C.M., et al., *Multilayered polyelectrolyte films promote the direct and localized delivery of DNA to cells.* J Control Release, 2005. **106**(1-2): p. 214-23.
5. Segura, T. and L.D. Shea, *Surface-tethered DNA complexes for enhanced gene delivery.* Bioconjug Chem, 2002. **13**(3): p. 621-9.
6. Segura, T., M.J. Volk, and L.D. Shea, *Substrate-mediated DNA delivery: role of the cationic polymer structure and extent of modification.* J Control Release, 2003. **93**(1): p. 69-84.
7. Segura, T., P.H. Chung, and L.D. Shea, *DNA delivery from hyaluronic acid-collagen hydrogels via a substrate-mediated approach.* Biomaterials, 2005. **26**(13): p. 1575-84.
8. Yoshikawa, T., et al., *Transfection microarray of human mesenchymal stem cells and on-chip siRNA gene knockdown.* J Control Release, 2004. **96**(2): p. 227-32.
9. Adler, A.F. and K.W. Leong, *Emerging links between surface nanotechnology and endocytosis: impact on nonviral gene delivery.* Nano Today, 2010. **5**(6): p. 553-569.

10. Bielinska, A.U., et al., *Application of membrane-based dendrimer/DNA complexes for solid phase transfection in vitro and in vivo.* Biomaterials, 2000. **21**(9): p. 877-87.
11. Bengali, Z. and L.D. Shea, *Gene Delivery by Immobilization to Cell-Adhesive Substrates.* MRS Bull, 2005. **30**(9): p. 659-662.
12. Jang, J.H., et al., *Surface adsorption of DNA to tissue engineering scaffolds for efficient gene delivery.* J Biomed Mater Res A, 2006. **77**(1): p. 50-8.
13. Pannier, A.K., B.C. Anderson, and L.D. Shea, *Substrate-mediated delivery from self-assembled monolayers: effect of surface ionization, hydrophilicity, and patterning.* Acta Biomater, 2005. **1**(5): p. 511-22.
14. Shen, H., J. Tan, and W.M. Saltzman, *Surface-mediated gene transfer from nanocomposites of controlled texture.* Nat Mater, 2004. **3**(8): p. 569-74.
15. Bengali, Z., J.C. Rea, and L.D. Shea, *Gene expression and internalization following vector adsorption to immobilized proteins: dependence on protein identity and density.* J Gene Med, 2007. **9**(8): p. 668-78.
16. Bonadio, J., et al., *Localized, direct plasmid gene delivery in vivo: prolonged therapy results in reproducible tissue regeneration.* Nat Med, 1999. **5**(7): p. 753-9.
17. Fang, J., et al., *Stimulation of new bone formation by direct transfer of osteogenic plasmid genes.* Proc Natl Acad Sci U S A, 1996. **93**(12): p. 5753-8.
18. Julkunen, I., T. Vartio, and J. Keski-Oja, *Localization of viral-envelope-glycoprotein-binding sites in fibronectin.* Biochem J, 1984. **219**(2): p. 425-8.
19. Williams, D.A., *Retroviral-fibronectin interactions in transduction of mammalian cells.* Ann N Y Acad Sci, 1999. **872**: p. 109-13; discussion 113-4.
20. Levy, R.J., et al., *Localized adenovirus gene delivery using antiviral IgG complexation.* Gene Ther, 2001. **8**(9): p. 659-67.

21. Honma, K., et al., *Atelocollagen-based gene transfer in cells allows high-throughput screening of gene functions.* Biochem Biophys Res Commun, 2001. **289**(5): p. 1075-81.
22. Steele, J.G., et al., *Adsorption of fibronectin and vitronectin onto Primaria and tissue culture polystyrene and relationship to the mechanism of initial attachment of human vein endothelial cells and BHK-21 fibroblasts.* Biomaterials, 1995. **16**(14): p. 1057-67.
23. Buck, C.A. and A.F. Horwitz, *Cell surface receptors for extracellular matrix molecules.* Annu Rev Cell Biol, 1987. **3**: p. 179-205.
24. Pankov, R. and K.M. Yamada, *Fibronectin at a glance.* J Cell Sci, 2002. **115**(Pt 20): p. 3861-3.
25. White, D.J., et al., *The collagen receptor subfamily of the integrins.* Int J Biochem Cell Biol, 2004. **36**(8): p. 1405-10.
26. Plow, E.F., et al., *Ligand binding to integrins.* J Biol Chem, 2000. **275**(29): p. 21785-8.
27. Rejman, J., A. Bragonzi, and M. Conese, *Role of clathrin- and caveolae-mediated endocytosis in gene transfer mediated by lipo- and polyplexes.* Mol Ther, 2005. **12**(3): p. 468-74.
28. Bathori, G., L. Cervenak, and I. Karadi, *Caveolae--an alternative endocytotic pathway for targeted drug delivery.* Crit Rev Ther Drug Carrier Syst, 2004. **21**(2): p. 67-95.
29. Sottile, J. and J. Chandler, *Fibronectin matrix turnover occurs through a caveolin-1-dependent process.* Mol Biol Cell, 2005. **16**(2): p. 757-68.
30. Rea, J.C., et al., *Engineering surfaces for substrate-mediated gene delivery using recombinant proteins.* Biomacromolecules, 2009. **10**(10): p. 2779-86.
31. McGavin, M.J., et al., *Fibronectin binding determinants of the Staphylococcus aureus fibronectin receptor.* J Biol Chem, 1991. **266**(13): p. 8343-7.

32. Boussif, O., et al., *A versatile vector for gene and oligonucleotide transfer into cells in culture and in vivo: polyethylenimine.* Proc Natl Acad Sci U S A, 1995. **92**(16): p. 7297-301.
33. Vecchione, R., et al., *Electro-Drawn Drug-Loaded Biodegradable Polymer Microneedles as a Viable Route to Hypodermic Injection.* Advanced Functional Materials, 2014. **24**(23): p. 3515-3523.
34. Ricoult, S.G., et al., *Generation of microisland cultures using microcontact printing to pattern protein substrates.* J Neurosci Methods, 2012. **208**(1): p. 10-7.
35. Miyazaki, T., et al., *The integrity of the conserved 'WS motif' common to IL-2 and other cytokine receptors is essential for ligand binding and signal transduction.* EMBO J, 1991. **10**(11): p. 3191-7.
36. Huff, S., et al., *Interaction of N-terminal fragments of fibronectin with synthetic and recombinant D motifs from its binding protein on Staphylococcus aureus studied using fluorescence anisotropy.* J Biol Chem, 1994. **269**(22): p. 15563-70.
37. Quinn, J.G., *Evaluation of Taylor dispersion injections: determining kinetic/affinity interaction constants and diffusion coefficients in label-free biosensing.* Anal Biochem, 2012. **421**(2): p. 401-10.